Applied Catalysis B: Environmental 336 (2023) 122891

Contents lists available at ScienceDirect

Applied Catalysis B: Environmental

journal homepage: www.elsevier.com/locate/apcatb

Design of modified MOFs electrocatalysts for water splitting: High current density operation and long-term stability

Yangping Zhang [a,b], Xiangjun Zheng [a], Xingmei Guo [a], Junhao Zhang [a], Aihua Yuan [a], Yukou Du [b,*], Fei Gao [a,*]

[a] School of Environmental and Chemical Engineering, Jiangsu University of Science and Technology, Zhenjiang 212003, PR China
[b] China College of Chemistry, Chemical Engineering and Materials Science, Soochow University, Suzhou 215123, PR China

ARTICLE INFO

Keywords:
Modified MOFs
Water splitting
High current density operation
Long-term stability

ABSTRACT

It is highly desirable to develop efficient catalysts under high-current-density operation and long-term stability for high performance water splitting. However, most reported modified MOFs catalysts exhibited favorable catalytic activity under a low current density on 10 mA cm^{-2} and limited stability. In response, reasonable design and applications modified MOFs catalyst with high current density and prolonged stability is essential yet challenging. In this review, we firstly summed the classifications of modified MOFs with pristine MOFs, MOFs composites and MOFs derivatives. Then, we discussed the strategies on the high-current-density activity improvement referring to the electronic structure tuning, defect construction and vacancy formation, and methods on the long-term stability enhancement including active sites protection, catalytic support reinforcement and efficient surface reconstruction. Finally, we proposed the challenges and prospects of modified MOFs to achieve improvement for further industrial water splitting, which could bring design principles in the field of modified MOFs materials.

1. Introduction

The ever-growing consumption of fossil fuels has caused a series of problems including environmental threat, energy crisis, and greenhouse effect. Therefore, developing next-generation energy technologies with cleanliness, sustainability, and zero carbon emission is high imperative [1–3]. Aiming at the global target of "carbon peaking and carbon neutrality", hydrogen, emerging as advanced high-density energy carrier (about 142 MJ kg^{-1}), has been considered as the ideal alternative to fossil fuels [4–6]. As one of the hydrogen production methods, water electrolysis has drawn intensive attention owing to the high efficiency, simplicity, pollution-free and energy security. However, both the two half reactions (anodic oxygen evolution reaction (OER) and cathodic hydrogen evolution reaction (HER)) require extra driving voltage to overcome the electrode and electrolyte resistance, resulting in high kinetic barriers with large overpotentials [7–9]. Moreover, the OER process with complex $4e^-$ transfer shows sluggish kinetic performance. Herein, it is urgent and essential to develop efficient electrocatalysts thus to improve the OER and HER performance for boosting the water splitting efficiency [10–12].

Up to now, the noble-metal-based nanomaterials are still regarded as the state-of-the-art electrocatalysts for electrochemical water splitting (EWS), such as the Pt-based catalysts for HER and Ru/Ir oxides catalysts for OER [13,14]. However, for one thing, the precious metals suffer from scarcity and fancy price. For another reason, the structural and composition instability, such as the dissolution of Ru phase and the formation of volatile high-valence Ru species in the Ru oxides catalysts for OER, could lead to the limited catalytic behaviors [15,16]. Consequently, it is imminent to explore cost-effective noble-metal-free catalysts with both high activity and durability to enhance the EWS performance. Meanwhile, the catalytic properties of reported noble-metal-free catalysts were mostly tested under a low current density of 10 mA cm^{-2} and displayed unsatisfied long-term stability, which is difficult to meet further industrial water electrolysis needs [17–19].

Although many noble-metal-free catalysts have displayed enhanced catalytic HER/OER behaviors with low overpotential under 10 mA cm^{-2}, owing to the deficient exposure of active sites and slow mass and electron transfer, making it difficult to achieve high current density [20–22]. Moreover, the electrooxidation and corrosion under high potential, as well as the exfoliation of catalytic materials from electrode

* Corresponding authors.
E-mail addresses: duyk@suda.edu.cn (Y. Du), gaofei006@just.edu.cn (F. Gao).

https://doi.org/10.1016/j.apcatb.2023.122891
Received 6 March 2023; Received in revised form 6 May 2023; Accepted 15 May 2023
Available online 18 May 2023

due to high-rate O_2 bubbles, could result in serve stability problems [23,24]. Therefore, designing robust large-current-density catalysts with long-term stability is highly desirable. Metal-organic frameworks (MOFs), emerging as advanced functional materials, possess merits of high porosity, rich metal open sites and high surface areas [25–27]. Researchers have designed many well-optimized MOFs catalysts to promote the OER/HER performance by pristine MOFs engineering, MOFs composites designing and MOFs derivatives construction. It is still desirable to develop MOFs catalysts working at the high current density (>200 mA cm^{-2}) and with long-term durability (10% variation of current density/operation voltage after 100-h stability tests) to approach the industrial demand.

Recently, a certain number of studies have reported the modified MOFs under high current density and long-term stability. Most reviews focus on the MOFs catalysts at a low current density of 10 mA cm^{-2}, while few reviews focus on the intrinsic profound promotion effect of modified MOFs catalysts under high-current-density operation for water splitting [28–30]. In this review, we summed the advanced modified MOFs as high-current-density catalysts for EWS and discussed the activity and stability origins from the modified MOFs materials. To be specific, we firstly discussed on the classifications of modified MOFs catalysts referring of pristine MOFs, MOFs composites and MOFs derivatives. Then, we analyze the requirements and activity promotion strategies involving electronic structure tuning, defect construction and vacancy formation for high-current-density operation, and investigate the requirements and approaches involving active sites protection, catalytic support reinforcement and surface reconstruction for long-term stability. Finally, we proposed the challenges and prospects in modified MOFs in further EWS developments.

2. Classification of modified MOFs catalysts

Up to now, researchers have designed many advanced strategies to synthesize modified MOFs catalysts, mainly including pristine MOFs by metal node engineering and ligand regulation, MOFs composites by MOFs@MOFs, LDH/MOFs, clusters/nanoparticles@MOFs, conductive polymer/MOFs and COFs@MOFs, and MOFs derivatives by MOF-derived oxides and oxyhydroxides, MOF-derived metal nitrides/phosphides/chalcogenides, and MOF-derived single-atom catalysts (Scheme 1). The synthesis and characteristics of those advanced MOFs catalysts have been summarized.

2.1. Modified pristine MOFs

Pristine MOFs are an important branch of MOFs nanocatalysts, which composed of metal ions or clusters linked by organic ligands. MOFs materials displayed the porous structures with good crystallinity, endow them with great potential in catalysis [31,32]. However, most un-modified MOFs materials suffer from lower percentage of available active sites and poor conductivity. For pristine MOFs nanomaterials, the catalytic active sites could be optimized by efficient tuning on metal ion centers and ligand fields, thus to improve the active sites density. Notably, the engineering on metal sites and ligand fields could avoid the agglomeration of metals and ligands, thus to remain the origin structure to the maximum [33,34]. Moreover, the surface coordinative unsaturated atoms and hydroxide ligands could be reserved. Herein, the

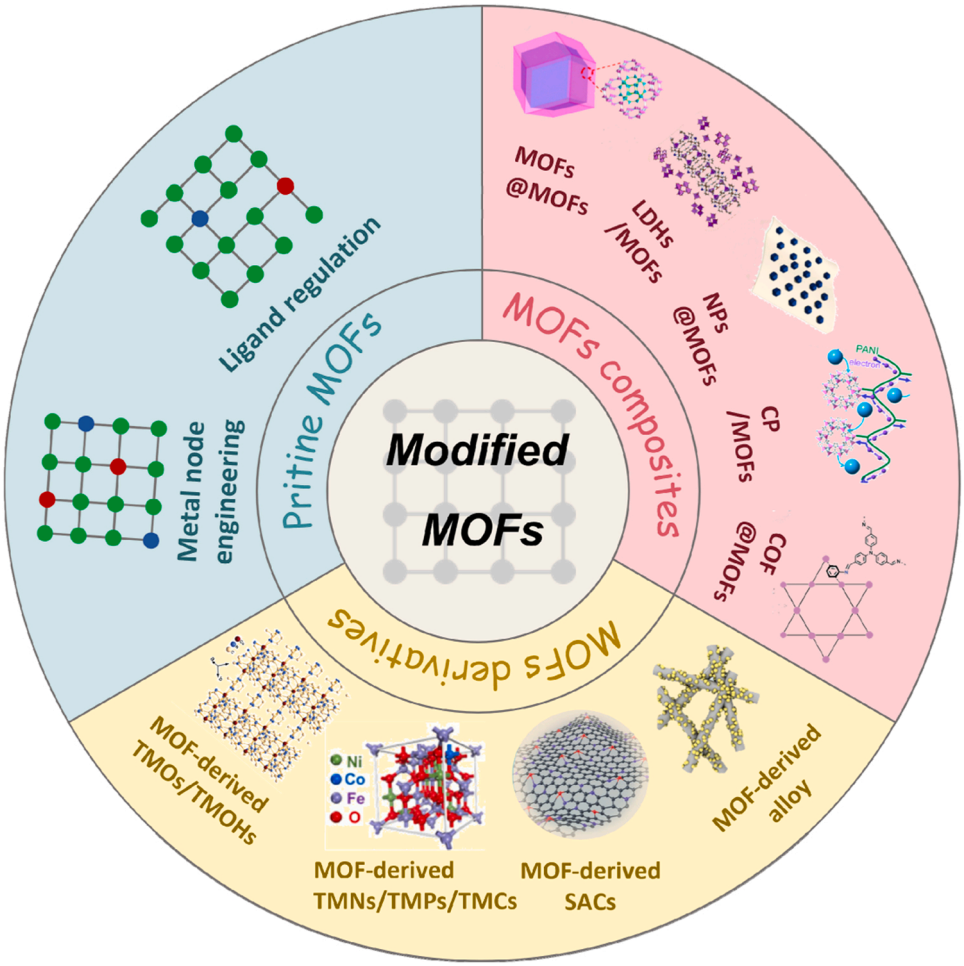

Scheme 1. Schematic illustration of classification of modified MOFs catalysts.

well-designed pristine MOFs could serve as robust heterogeneous electrocatalysts due to the electronic and synergistic effect, as well as porous channels for accessible active centers.

2.1.1. Metal node engineering

Most MOFs materials are constituted by non-noble transition metals (Fe, Co, Ni, Cu, Zn, etc) and organic linkers. The non-noble transition-metal-based nanomaterials have been considered as promising alternatives of noble-metal catalysts in water splitting [35,36]. Meanwhile, the metal sites, especial for the unsaturated metal sites are recognized as the active centers in HER/OER processes. Engineering the metal ion sites from monometallic sites to bimetallic, trimetallic, and even multi-metallic sites by partial substitution is an efficient yet facile method to modify the pristine MOFs [37].

The solvothermal method is a mostly-used strategy to prepare MOFs materials, which could also realize the tuning on metal ion sites by simply introducing a second metal that differs the original metal in the frameworks as co-starting metal precursors. In Fig. 1a, Lang et al. have reported a class of Fe/Ni-based trimetallic MOFs (Fe/Ni/Co(Mn)-MIL-53) nanocatalysts [38]. The Fe-MIL-53 frameworks were composed of 1, 4-bezenedicarboxylate (1,4-BDC) and FeO_6 octahedrons. The Fe sites could be partially replaced by Ni ions while maintaining the one-dimensional construction (Fig. 1b and c). In addition, the introduction of a third metal (Co or Mn) could also keep the framework and strengthen the synergistic effect by tuning the electronic interaction. In addition to the solvothermal method (bottom-up), Zhu and co-works have developed another novel "oxide-sacrifice" way (up-bottom) to realize the control on metal ion nodes in flexible combination (Fig. 1d) [39]. This method adopted amorphous FeCo oxides nanosheets as starting materials to synthesize ultrathin MOF-74 nanosheets via confined ligand coordination. Differ from the solvothermal strategy, this advanced method could not only avoid the aggregation of organic modulators on MOFs surface for blocking the active sites, but also realize the large-scale preparation. In addition, a set of monometallic and bimetallic MOF nanosheets were obtained, indicating the universality of this method.

The above-mentioned common solvothermal method and specific "oxide-sacrifice" show their advantages and scope of applications. It should be pointed that the simplicity and generality of those strategies were beneficial for the synthesis of MOFs, which is expected to promote further improvement for practical proton exchange membranes water electrolyze (PEMWE) under high current density [40,41]. Not only for various synthetic methods for MOFs with mixed metal nodes, the metal valence engineering is also a robust approach to modifying MOFs

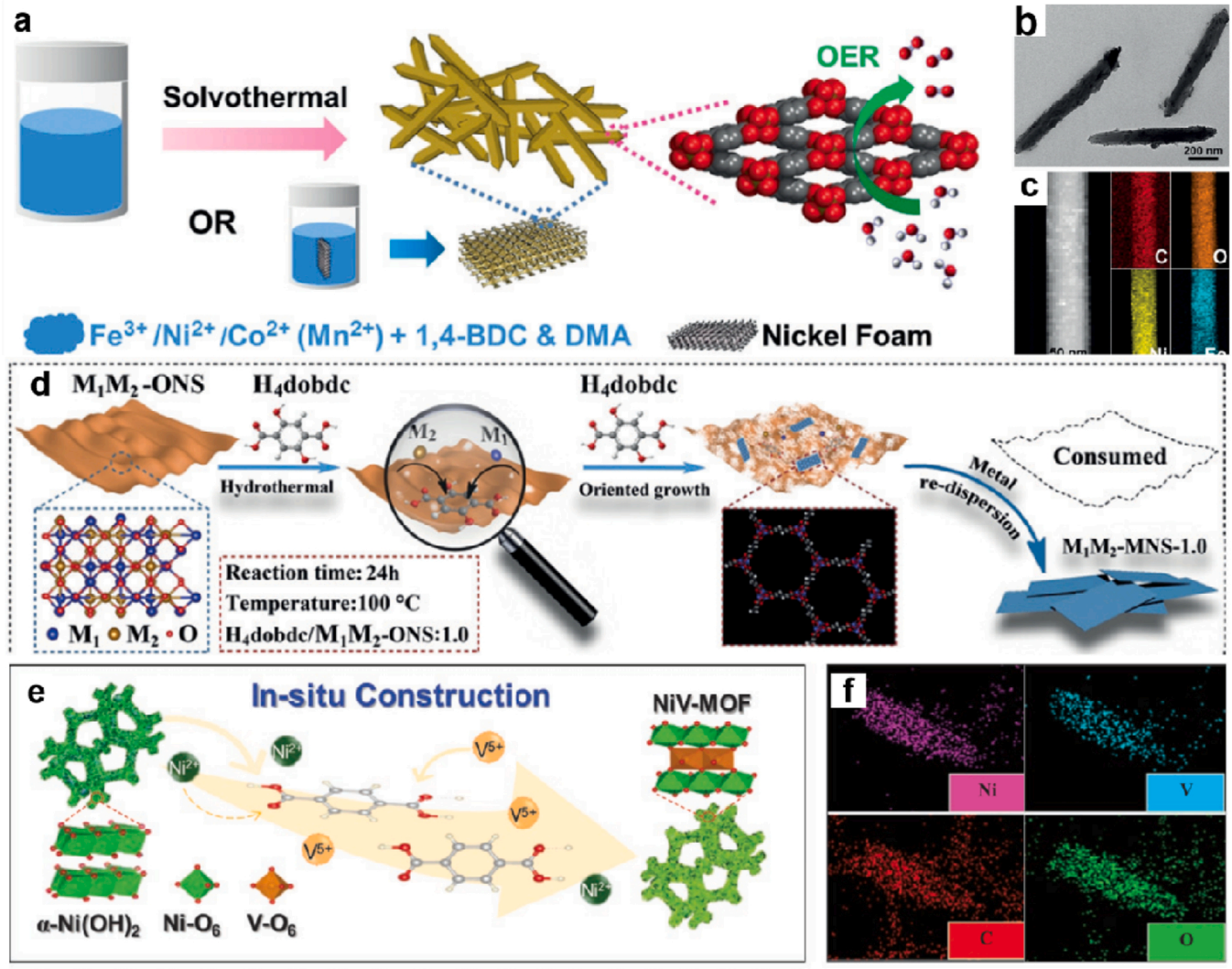

Fig. 1. (a) Schematic image of the preparation of Fe/Ni/Co(Mn)-MIL-53 and Fe/Ni/Co(Mn)-MIL-53/NF, (b) TEM image and (c) HAADF-STEM image and STEM-EDS mapping images of $Fe/Ni_{2.4}$-MIL-53, (d) schematic image of the "oxide-sacrifice" approach to form M-MNS, (e) schematic image of in situ construction of flexible V-Ni redox centers into NiV-MOF NAs and (f) EDS mapping images of NiV-MOF NAs. (a-c) Reprinted with permission from Ref. [38]. Copyright (2017) Wiley-VCH. (d) Reprinted with permission from Ref. [39]. Copyright (2019) Wiley-VCH. (e and f) Reprinted with permission from Ref. [42]. Copyright (2021) Wiley-VCH.

catalysts at an atomic level. Liu et al. have proposed an in-situ method to construct a flexible V-Ni redox centers by introducing vanadium with multiple elemental states (Fig. 1e) [42]. The EDS mapping images confirmed the successful introduction of V elements in NiV MOFs catalysts (Fig. 1 f). The unique electronic configuration of V could offer flexible metal states of $V^{+3/+4/+5}$, with $Ni^{+3/+4/+5}$, forming V-Ni sites to optimize electronic structures in NiV MOFs. The metal valence engineering also provides an important reference in pristine MOFs modification.

2.1.2. Ligand regulation

As another important component in MOFs, the modification on organic linkers also has an impact on the variations of the physicochemical properties. Owing to the diversity of organic linkers, MOFs families including zeolitic imidazolate frameworks (ZIFs), Materials of institute lavoisier (MIL), carboxylate-based MOFs, porphyrin-based MOFs, and etc have attracted intensive attention [43–45]. Meanwhile, the ligand regulation, such missing linker, functionalized linkers, competitive coordination, and other strategies have been developed, overcoming the shortcomings of pristine MOFs, endowing with excellent properties.

It is confirmed that the topological structure and coordination states have an influence on the electronic structure of MOFs. Researchers have introduced missing linkers into MOFs structures to tune the electronic environments. Li and co-workers have realized the preparation of missing-linker MOFs via introducing different missing linkers into Co-BDC (Fig. 2a) [46]. Similar as Co-BDC, the Co-BDC-Fc (Co-BDC with missing linker carboxyferrocene) still showed a stable two-dimensional nanosheets structures, maintaining the MOFs structures well (Fig. 2b and c). The DFT calculations reflected that the Co-BDC with missing linkers demonstrated a more conductive electronic structure with optimized electronic state near Fermi level. This work adopted Fc to introduce missing linker, other methods such as microwave-induced plasma engraving has reported as well.

Differ from the missing linker introduction, the functional linkers regulation has become a robust strategy to modify pristine MOFs materials. For the organic linker, the functional groups, such as $-NH_2$, -OH, -Br, and $-OCH_3$ could be introduced to change the surficial properties involving hydrophilia and wettability [47,48]. The defect stain and binding energy of pristine MOFs materials could also be tuned. For example, Fisher's group has introduced diverse functional groups X (X = -Br, $-OCH_3$, and $-NH_2$) to BDC to generate various NiFe MOFs by alkaline treatments (Fig. 2d) [49]. The Raman spectroscopy and XPS have seen the evolution of lattice distortion and defect strain in MOF with BDC-X. Moreover, other pristine MOFs with functional groups, such as Cu-Fe-NH_2 MOF, have been reported [50].

2.2. Modified MOFs composites

The controllable synthesis of MOFs composites has generated many kinds of MOFs composites by integrating pristine MOFs with other different functional nanomaterials. The obtained MOFs composites were composed of MOFs and other diversified components, including MOFs@MOFs, layer double hydroxide (LDH)/MOFs, cluster/nanoparticle@MOFs, conductive polymer/MOFs, and covalent organic framework (COF)/MOFs. These well-modified MOFs composites show

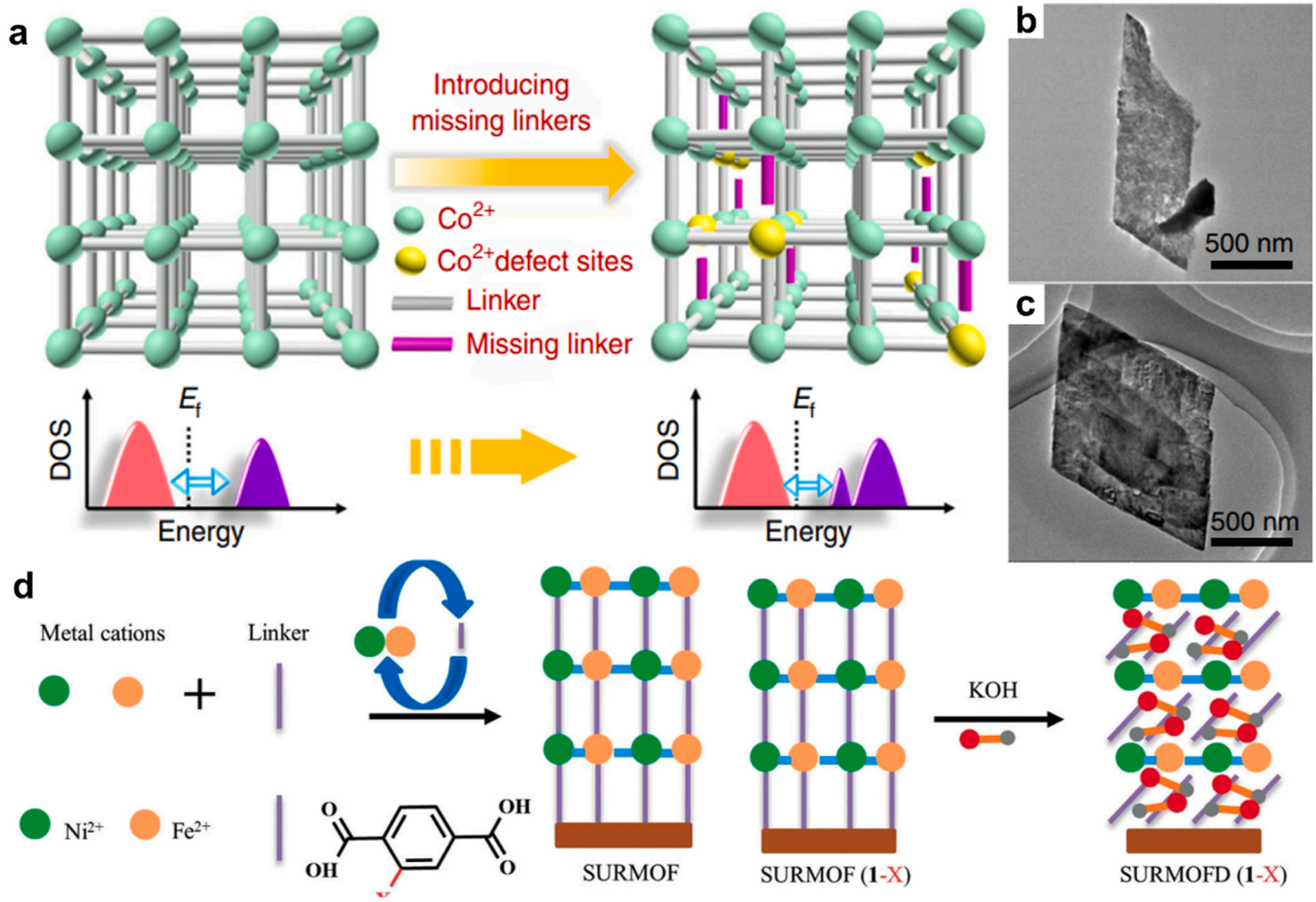

Fig. 2. (a) Modulating electronic structure of MOFs via introducing missing linkers for OER, TEM images of (b) CoBDC-NF and (c) CoBDC-Fc–NF, (d) preparation of NiFe-BDC (X) SURMOFs (X = NH_2, H, OCH_3 and Br). (a-c) Reprinted with permission from Ref. [46]. Copyright (2019) Nature Publishing Group. (d) Reprinted with permission from Ref. [49]. Copyright (2020) Wiley-VCH.

combined advantages of MOFs and the counterpart function materials, thus to display benign structural flexibility and adaptability, high porous and structure of MOFs, as well as the specific merits of functional materials [51,52]. The modified MOFs composites are expected to display superior catalytic behaviors, which possessed enormous potential to apply in the high-current-density water splitting.

2.2.1. *MOFs@MOFs composites*

It is determined that there is a close relationship between different MOFs materials. The modified MOFs@MOFs composites tend to show plural characteristics differ from individual MOFs nanomaterials [53]. The MOFs@MOFs composites usually possess core@shell structures with robust synergistic effect. The complex structures could improve the conductivity, optimize the porosity, and enhance the structural stability, making MOFs@MOFs composites become promising catalytic materials [54,55].

For the construction of MOFs@MOFs, Dou et al. have reported a simple stepwise method to synthesize Ni-MOF@Fe-MOF composites (Fig. 3a) [56]. The Fe-MOF nanoparticles were deposited on Ni-MOF nanosheets. The synergistic effect between Ni active centers and Fe species could be strengthen in this MOF@MOF hybrid composites. Notably, this work realized the single deposition of MOFs on matrix MOFs. The multiple MOFs@MOFs composites have been reported as well. Yu's group has designed a series of ternary MOF@MOF heterostructures by using MIL-125 as a starting material (Fig. 3b) [57]. Under the guideline of the in-situ multiple selective assembly strategy, a set of ternary hybrid MOFs structures including MIL-125 @ZIF-67 @ZIF-8 (type A), MIL-126 @ZIF-8 @ZIF-67 (type B) and MIL-126 @ZIF-8 @Zn, Co-ZIF (type C) have been obtained. This unique selective growth method not only guide different MOFs materials into a hybrid MOF

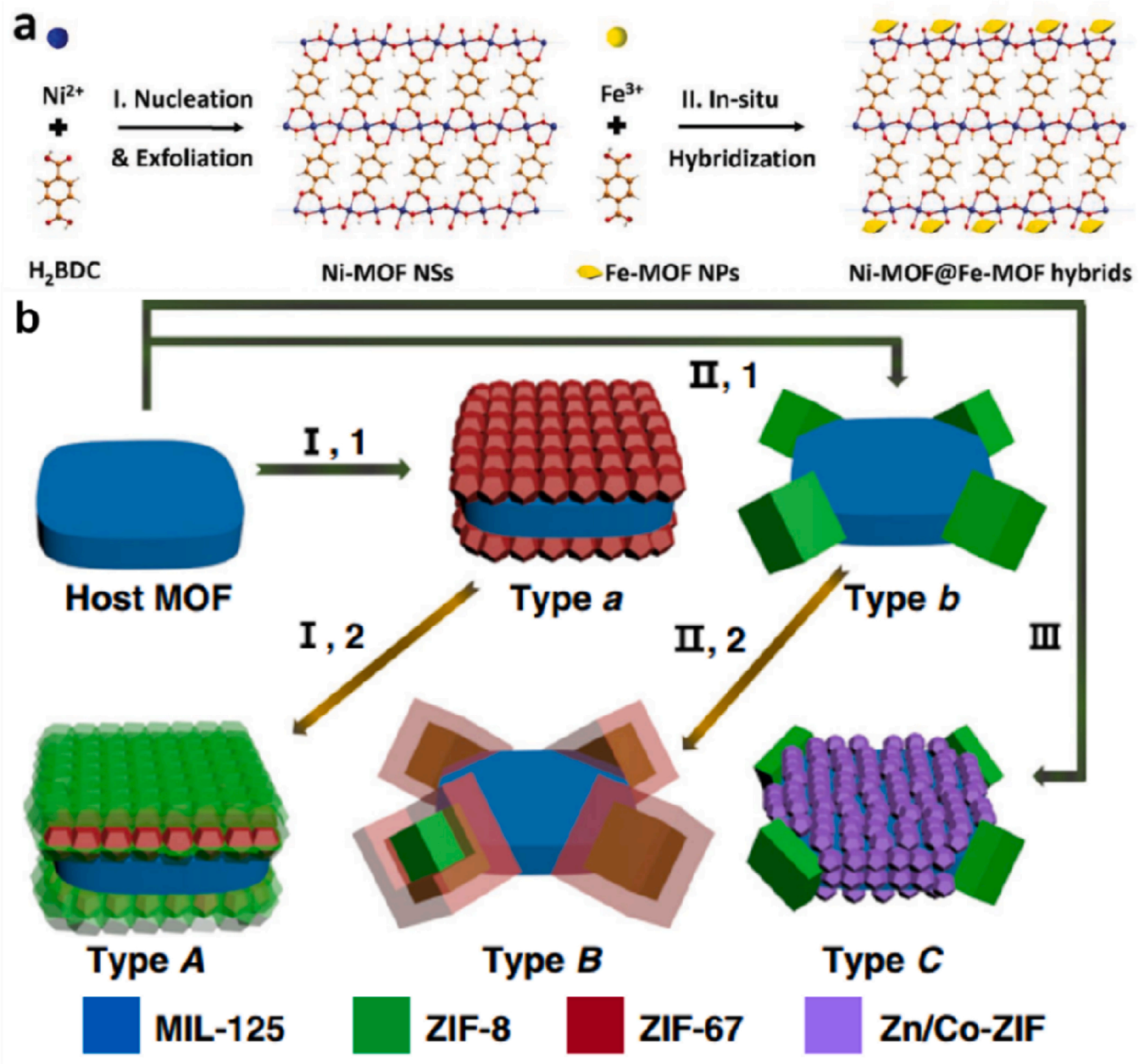

Fig. 3. (a) Schematic image of synthesis of Ni-MOF@Fe-MOF hybrid nanosheets. (b) Schematic image of the multiple synthesis approaches (I-III) and structures of ternary MOF-on-MOF heterostructures (types A-C). (a) Reprinted with permission from Ref. [56]. Copyright (2018) Wiley-VCH. (b) Reprinted with permission from Ref. [57]. Copyright (2020) Nature Publishing Group.

assembly with structural and compositional complexity, but also provide instructive reference for other synthesis on advanced MOFs@MOFs composites. Other MOFs@MOFs materials such as Co-BPDC@Co-BDC heterojunction, NH_2-MIL-125 @ZIF-67, and etc have been prepared [58,59].

2.2.2. *LDH/MOFs composites*

Layer double hydroxides (LDHs) are the typical 2D materials with the general formula of $[M^{2+}_{1-x}M^{3+}(OH)_2]^{x+}(A^{n-})_{x/n}\bullet mH_2O$. LDHs show the brucite-like layered flexible construction with high surface areas and adjustable components, offering convenient tunnels for electron transfer and mass transportation [60]. However, LDHs possess the inherent drawbacks with stacked and overlapped structures, which lead to more covered metal active sites without sufficient exposure. The metal sites in MOFs are uniformly distributed, which could offer large numbers of dispersive yet abundance active metal sources [61–63]. The combination of targeted LDH and MOFs could alleviate the self-agglomeration effect of LDH, expose more potential metal active sites, and thus to improve the conductivity, durability, and reactivity of LDH/MOFs composites [64].

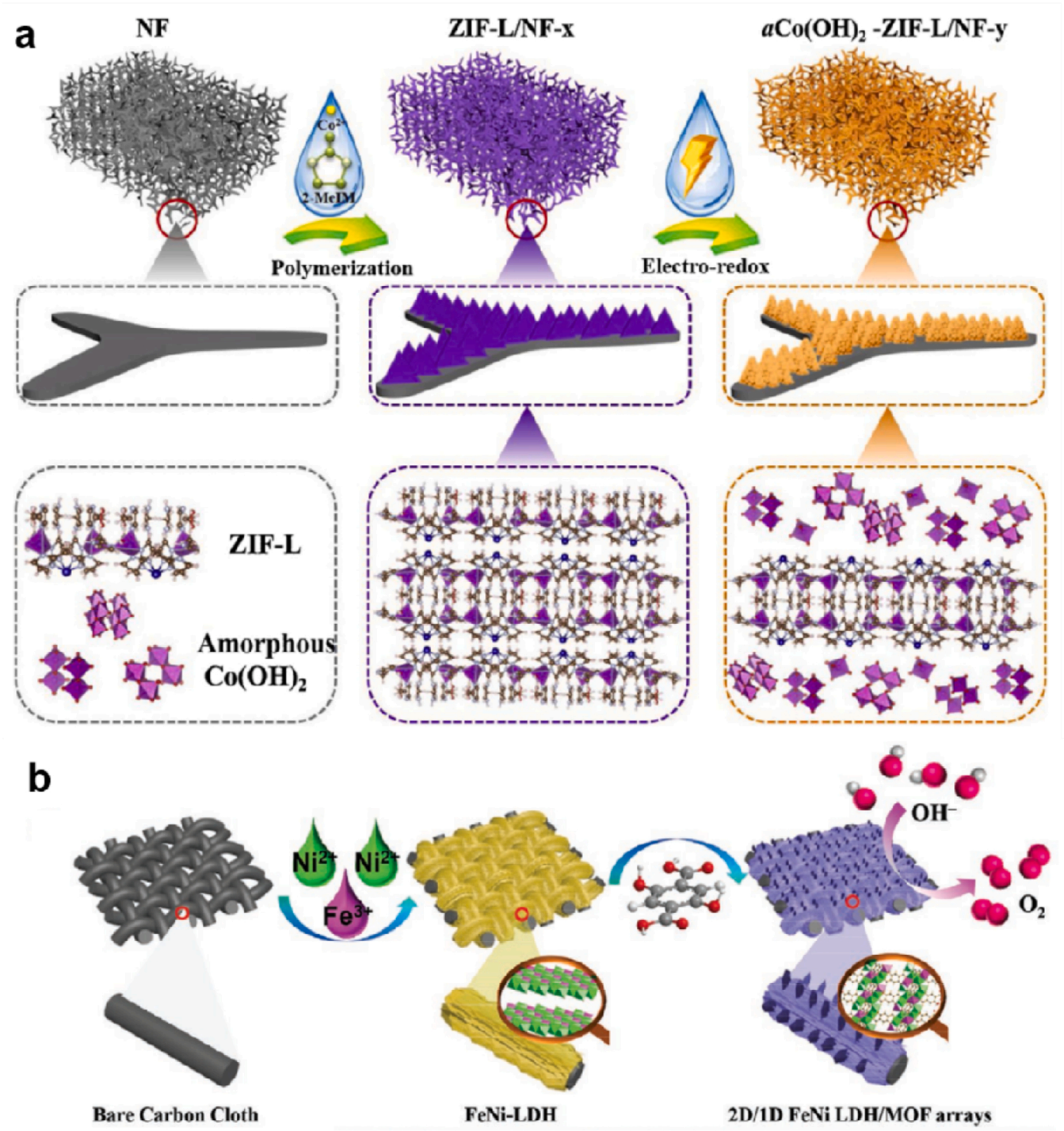

Fig. 4. (a) Schematic image of the synthesis of ZIF-L/NF-x and a$Co(OH)_2$-ZIF-L/NF-y and (b) Schematic illustration of the preparation of 2D/1D FeNi LDH/MOF arrays. (a) Reprinted with permission from Ref. [66]. Copyright (2021) Elsevier. (b) Reprinted with permission from Ref. [67]. Copyright (2021) Wiley-VCH.

Many strategies have developed to prepare LDH/MOFs composites, one simple and rational approach is in-situ transformation. Zhai's group has engineered a universal method to achieve a transformation to prepare hierarchical LDH/MOF composites [65]. The Fe-Ni LDH nanosheets were generated from the FeNi-MOF-74 by alkali treatment. Notably, the MOFs could totally convert into Fe-Ni LDH by continuous treatment. The Fe-Ni LDH/MOFs exhibited a hollow columnar-like bracket structure anchored by many LDH nanosheets. This modified LDH/MOFs composites exhibited rich metal sites and extended electronic transport channels. Differ from the alkali treatment, the electrochemical method could act as another approach to convert LDHs in MOFs materials. In Fig. 4a, Li et al. have designed a general in-situ synthesis to convert CoM-ZIF-L precursors to amorphous $Co(OH)_2$/ZIF-L catalysts by adopting cyclic voltammetry (CV) redox way [66]. The CV redox process could activate the reversible redox of metal ions and remove the ligands and then capped OH^-. Then, the defective amorphous hydroxides were formed. It has been confirmed that the modified $Co(OH)_2$/ZIF-L catalysts possessed abundant catalytic centers, enhanced conductivity and fast ion diffusion routes.

In addition to the in-situ transform routes by taking MOFs as semi-sacrificial template via chemical or electrochemical driving, the evolutions from LDH to MOFs by using LDH as template have also been attempted. In Fig. 4b, Chen's group have constructed a kind of 2D FeNi LDH nanosheets packed with 1D FeNi MOFs catalysts [67]. The FeNi LDH nanosheets were firstly formed with tunable orientation of active centers and edge-open octahedral MO_6 layer-stacking architecture, which facilitated the further growth of Fe-Ni MOFs. The LDH/MOFs composites offered the robust amorphous/crystalline interface and 2D–1D dimensional-combined structure, playing a significant role in catalytic reactions. This kind of modified LDH/MOFs composites,

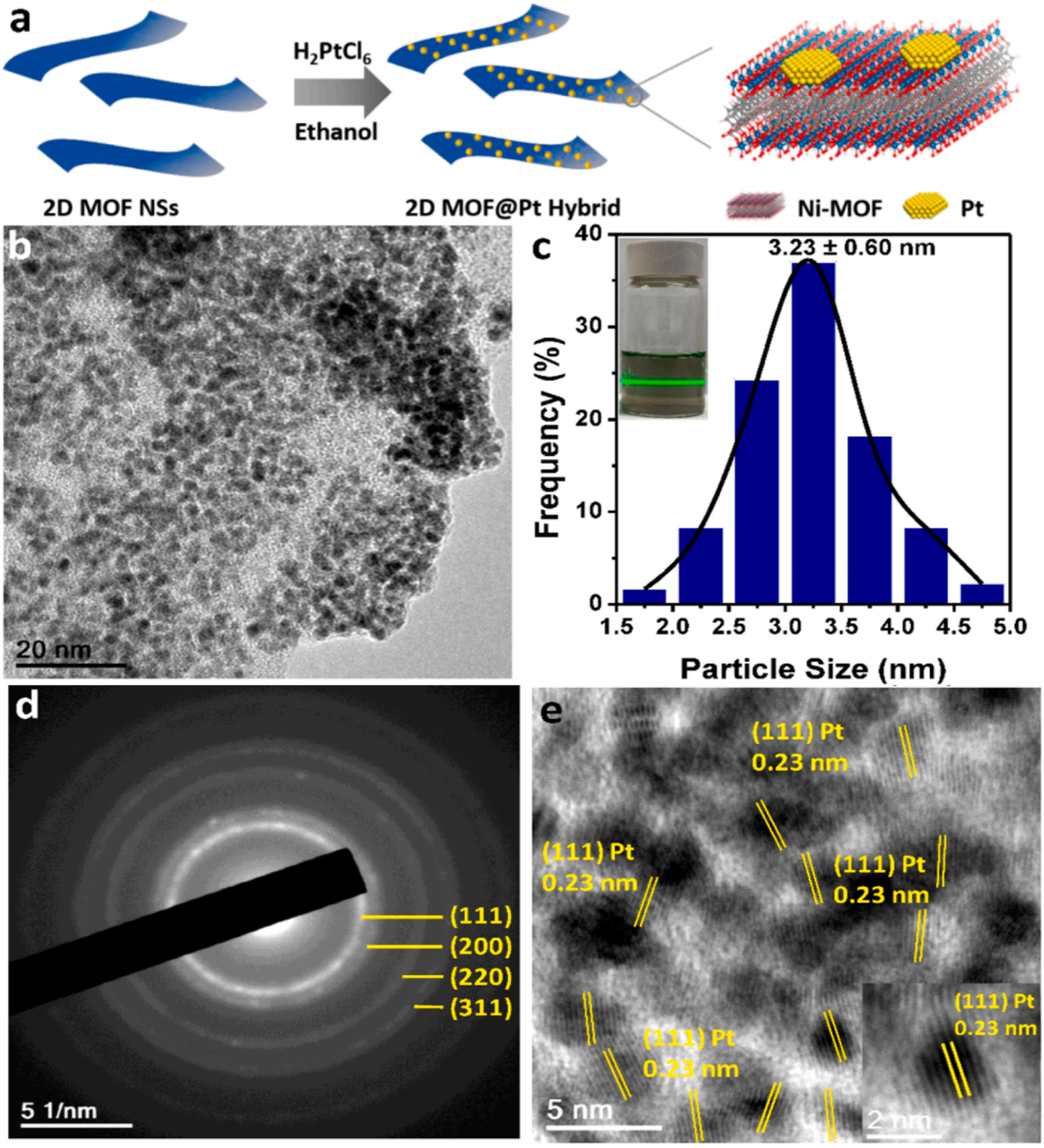

Fig. 5. (a) Schematic illustration of the synthesis on 2D MOF@Pt, (b) TEM image of 2D MOF@Pt nanosheet, (c) size distribution of Pt NPs on on 2D MOF nanosheets (insert the digital image), (d) SAED pattern and (e) HRTEM image of 2D MOF@Pt nanosheets. (a-e) Reprinted with permission from Ref. [73]. Copyright (2019) American Chemical Society [73]. (f) Reprinted with permission from Ref. [74]. Copyright (2020) Wiley-VCH.

including many other reported catalysts, serving as high-performance catalysts in high-current-density water splitting.

2.2.3. Nanoparticle@MOFs composites

Among MOFs composites families, nanoparticles have been demonstrated as robust partners. By introducing extrinsic or in-situ formed functional cluster or nanoparticles species, the heterogeneous structures are usually constructed with new properties [68–72]. For cluster/MOFs composites, Li et al. have introduce the metal sulfide (MS) clusters into FeNi MOFs on nickel foam and to form the NiFe-MS/MOF@NF catalysts by one-pot method (Fig. 5f) [73]. It has been confirmed that the MS cluster facilitated the formation of ultrathin MOF nanosheets, which could optimize the adsorption energy of intermediates for accelerated catalytic behaviors.

For nanoparticles (NPs), especial for noble metal NPs, they usually exhibited fascinating functionality and tunable properties. Sun's group has designed a kind of direct hybridization method to synthesize noble metal/2D MOF heterojunctions catalysts (Fig. 5a) [74]. The Pt NPs were formed in Ni-MOFs nanosheets (Fig. 5b), meanwhile, the Ni MOFs offer the rich anchoring sites for Pt deposition. The TEM images displayed the uniform distribution of Pt NPs with the average size of 3 nm (Fig. 5c). The SAED pattern revealed the diffraction rings, corresponding to the characteristic planes of Pt (Fig. 5d). The lattice spacing of Pt NPs was measured as 0.23 nm (Fig. 5e). The NPs@MOFs hybrid structure was expected to enable desirable interface synergistic effect by strengthening metal-O interaction. Not only for the Pt NPs@MOFs, even PtNi alloy@MOF, site-anchored Pt@MOF have also been reported [75,76]. This kind of modified hybrids pave new way for the synthesis of functional cluster/nanoparticle@MOFs composites.

2.2.4. Conductive polymer@MOFs composites

Conductive polymer is a kind of organic materials with superior conductivity, mainly involving polyanilines (PAN), polypyrroles (PPy), polythiophenes, etc. CPs usually exhibit satisfied thermal durability, chemical stability, and high mechanical flexibility [77]. The metal-N bonds derived from rich N sources in CPs would also generate by constructing modified CPs@MOFs composites, while the M-N sites, such as Co-N_4 sites, have been confirmed as the active sites. Hence CPs@MOFs composites catalysts are expected to display high conductivity and activity [78,79].

Yang's group have designed an advanced FeNi-PPy composites by in-situ polymerization (Fig. 6a) [80]. The FeNi-MIL-88 precursors were synthesized by a solvothermal method, which presented a distinct spindle structure (Fig. 6b). Then, the pyrrole was added and self-polymerized on the FeNi-MIL-88, and form the FeNi-PPy composites with hollow spindles (Fig. 6c). The FeNi-PPy composites could confine the reactants into a certain surrounding to add the collision frequency to active the catalytic reactions. In addition, the N in PPy could lower the variation of free energy of the intermediates during the reaction steps, which serve as promising candidates in large-current-density water splitting. In addition, Deng' group have fabricated a kind of CPs/MOFs composing ZIF-67 and polyacrylonitrile [81]. The fabric electrode possesses the properties of both stability and flexibility, playing important role on the catalysis. More CPs/MOFs such as Fe/NCNFs and ZIF-8 @ZnO/PAN were reported as well [82,83].

2.2.5. COF/MOFs composites

Covalent-organic frameworks (COFs) were firstly discovered in 2005, which are a kind of extended crystalline organic materials with rigid backbone, long-range ordered and permanent porosity [84].

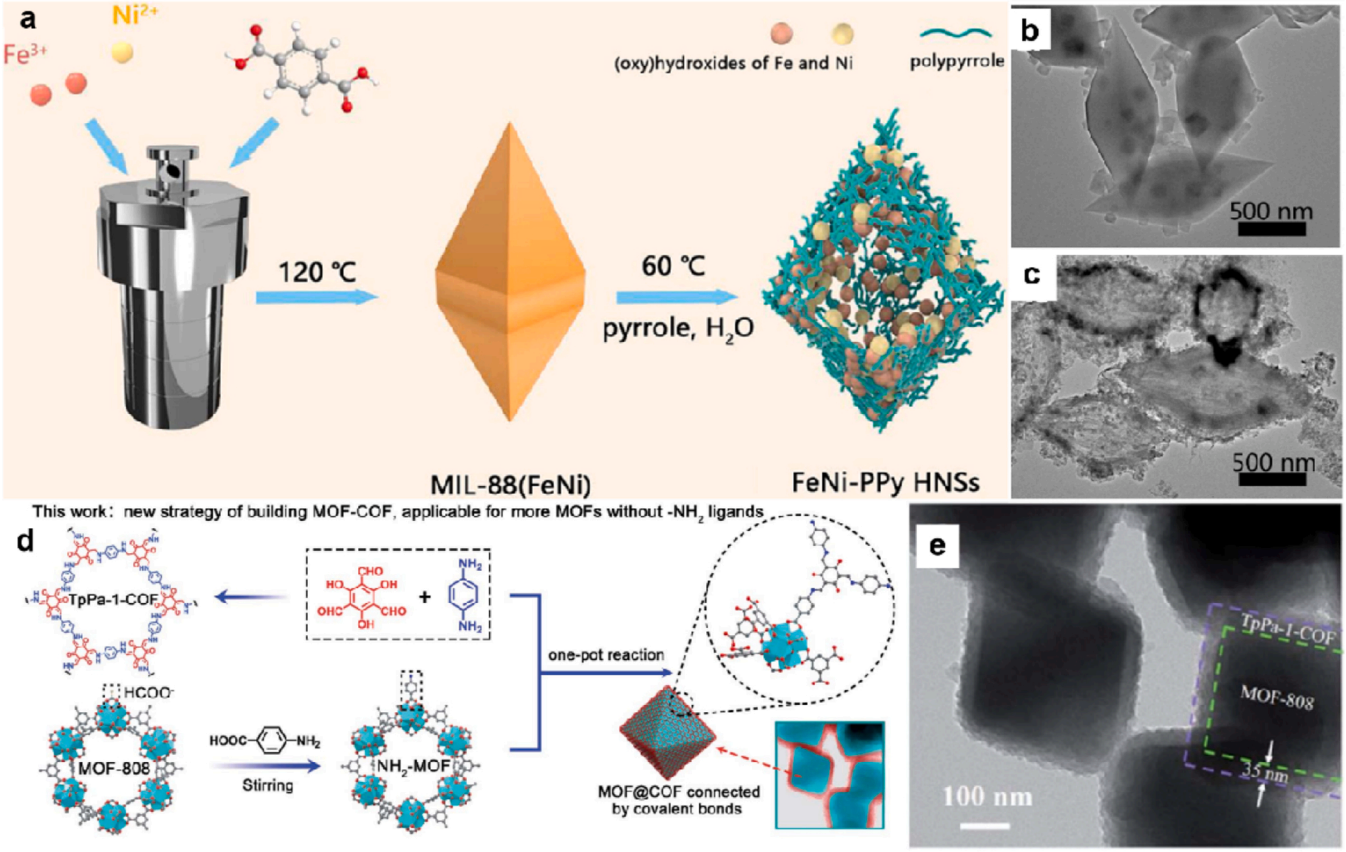

Fig. 6. (a) Schematic image of the preparation on FeNi-PPy HNSs, (b) TEM images of MIL-88(FeNi) and (c) FeNi-PPy HNSs, (d) schematic image of MOF@COF hybrid materials and (e) TEM image of MOF-808 @TpPa-1-COF. (a-c) Reprinted with permission from Ref. [80]. Copyright (2020) Elsevier. (d and e) Reprinted with permission from Ref. [89]. Copyright (2021) Royal Society of Chemistry.

However, it is difficult that mono COFs materials applied as catalysts directly due to the absence of catalytic active metal sites in COFs. Meanwhile, the MOFs materials were rich in metal centers. The COF/-MOF composites were believed to generate more fantastic properties [85,86]. Specifically, the COFs with good conductivity could improve the conductivity of obtained COF/MOFs composites; COFs featuring fast electron transfer could enhance the electrochemical behaviors of COF/MOFs composites; The surface areas and pore volumes could also be enlarged thanks to the rational combination of COFs and MOFs [87, 88]. In addition, the high chemical stability of COFs would make up the deficiency of environmental instability of MOFs. Herein, it is desirable to develop and modify functional COF/MOFs composites catalysts.

Yan et al. have designed a typical covalent connect MOF-COF hybrid materials of core-shell MOF-808 @TpPa-1-COF [89]. As shown in Fig. 6d, the MOF-808 was firstly prepared by a stirring route. Afterwards, the pristine MOFs were modified by -NH_2 groups to generate NH_2-MOF-808. Finally, the NH_2-MOF-808 precursors were introduced into the TpPa-1-COF solution to fabricate the MOF-COF composites. In Fig. 6e, TEM image of MOF-808 @TpPa-1-COF revealed the distinct core-shell structures where MOF-808 as core and TpPa-1-COF as shell. In detail, the thickness of shell structure was determined as about 35 nm. The versatility of obtained MOF/COF materials could be well verified. Not only for the above hybrid materials, other advanced MOF/COF composites have been synthesized [90].

2.3. Modified MOFs derivatives

The modification on pristine MOFs and MOFs composites was based

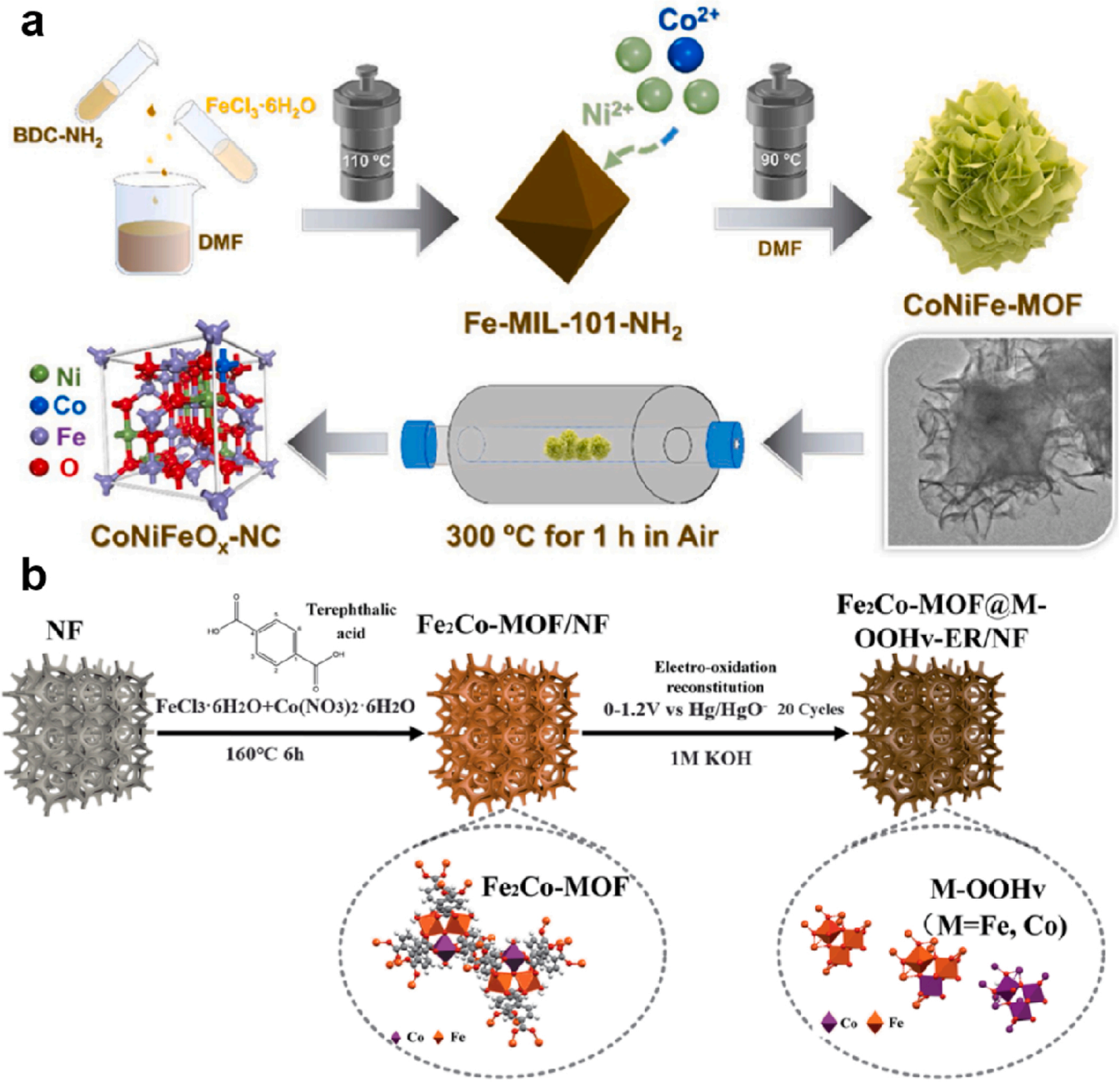

Fig. 7. (a) Schematic for the synthesis on $CoNiFeO_x$-NC from Fe-MIL-101-NH_2 MOFs. (b) Schematic image of the in situ synthesis on Fe_2Co-MOF@M-OOHv-ER/NF. (a) Reprinted with permission from Ref. [103]. Copyright (2021) Elsevier. (b) Reprinted with permission from Ref. [107]. Copyright (2021) Royal Society of Chemistry.

on the original MOFs under relative mild environment such alkali process, while the total or partial MOFs structures could be preserved. Different from the above designing, MOFs derivatives are usually prepared after high temperature calcination, hardly keep the MOFs architecture [91,92]. Generally, the MOFs are usually served as precursors or templates. After targeted postprocessing treatments including calcination, sulfuration, phosphorization, and etc, the objective various MOFs derivatives could be obtained, including MOF-derived oxide, oxyhydroxide, chalcogenides, phosphide, nitride, and N-doped C materials [93,94].

A wide range of this modified MOFs derivatives have been reported, which were verified to possess prominent characters and advantages. The synthesis of MOF-derived oxide and oxyhydroxide benefits to the introduction of defects structure with more active sites [95,96]; The hetero-atoms such as P, S and Se in MOF-derived chalcogenides/phosphide/nitride could tune the binding energy of active species in catalytic reactions [97,98]; The MOF-derived N-doped C materials could also not only act as functional conductive materials thus to directly become efficient catalysts, but also provide robust support or host to anchor the single atom catalysts (SAC) thus to boost the catalytic behaviors [99,100]. Considering that the common MOF derivatives such as mono derivatives have been largely reported. This section would mostly focus on the modified MOF multi-derivatives and other advanced SAC/MOF derivatives, mainly including MOF-derived oxide/oxyhydroxide, MOF-derived chalcogenides/phosphide/nitride, and SAC/MOF-derived N-doped C materials.

2.3.1. MOF-derived oxides and oxyhydroxides

MOF-derived oxides catalysts were often prepared by calcinating the modified MOF precursors in air. For the robust water splitting catalysts, transition-metal-based (Fe, Co, Ni) MOFs materials are ideal precursors to fabricate efficient transition metal oxides (TMOs) catalysts [101,102]. Researchers have engineered many strategies including compositional tuning, morphology control and active species cooperation to enhance the catalytic behaviors. Zhang's group have synthesized the hierarchical Co-Ni-Fe oxides catalysts derived from MOFs [103]. In Fig. 7a, the pristine Fe-MIL-101-NH_2 were firstly obtained. Then, the CoNiFe MOFs were obtained after ion-exchange. Finally, the CoNiFeO_x-NC catalysts were synthesized after pyrolysis. The prepared CoNiFeO_x-NC catalysts displayed the octahedral structures surrounded by some fluffy nanosheets. The Co^{2+} could etch the surface of pristine MOFs while the Ni^{2+} participated in the construction of nanosheets. The pyrolysis could promote the redistribution of electrons and thus lower the energy level in catalytic reactions, imply the indispensable role of constructing robust oxides. Not only for this trimetallic oxides materials, other well-modified MOF-derived oxides catalysts have been been reported as well [104].

Differ from the synthesis on MOF-derived oxides, the controllable oxidation of MOFs precursors could contribute to the formation of MOF-derived oxyhydroxides [105]. More importantly, the metal oxyhydroxides (M-OOH) are usually confirmed as the practical active sites in OER process. The rational modify on M-OOH has a great impact on the intrinsic activity enhancement. The conventional oxidation process consumes much energy accompanied with some products in low-purity, which is difficult to obtain highly-purified targeted products [106]. Yu' group have adopted a novel in-situ electrooxidation method to prepare the Fe_2Co-MOF@M-OOH_v-ER/NF catalysts (Fig. 7b) [107]. The formation of M-OOH could introduce oxygen defect and improve synergistic effect to the catalysts for superior catalytic performance.

2.3.2. MOF-derived metal nitrides/phosphides/chalcogenides

Apart from the MOF-derived oxides/oxyhydroxides, other MOF-derived metal nitrides, phosphides, and chalcogenides with intricate structures have been widely reported for water splitting [108]. Different from the TMO and M-OOH, the heteroatoms including N, S and P exhibited high electronegativity and different electronic structures, play indispensable role on the catalytic reactions [109,110].

Specifically, for MOF-derived transition metal nitrides (TMNs), the N atoms with small radius often occupy the band gap position of metal lattice, thus to display the distinct metal-like properties involving high melt and boiling point and superior electrical conductivity [111]. Up to date, the synthesis on TMNs was limited to the N sources supply. Although N atoms are abundant in ligands, the addition N sources (such as NH_3) are still needed [112]. For MOF-derived transition metal phosphides (TMPs), the TMPs possess the metallicity and large surface areas. The P atoms could facilitate the in-situ formation of hydroxides and oxyhydroxides on the catalytic surfaces and generate more coordinative active sites. The synthesis strategies of TMPs are relatively mature. The phosphating process could be operated by calcination temperature about 200–400 ℃ under inert atmosphere. PH_3 gas produced by upwind pyrolysis of NaH_2PO_2 is used to react with downwind MOFs to prepare TMPs [113,114]. MOF-derived metal chalcogenides included transition metal phosphides (TMSs) and transition metal selenides (TMSes). TMSs have similar physical and chemical properties with TMPs. According to different S sources, the synthetic methods of TMSs are various, including calcinating sulfidation, liquid sulfidation and in-situ sulfidation, which provide more possibilities for the development of high-performance water splitting catalysts [115]. As another member in MOF-derived metal chalcogenides, TMSe possess relative weak chemical bonds due to the small electronegativity, which exhibit high conductivity. The phase types of TMSe were various with the different Se amounts. Hence there may be more choices when adjusting their electrochemical performance [116,117]. Similarly, the solid phase and liquid phase methods were also be adopted to realize the synthesis of MOF-derived selenides.

On account of the above understanding, lots of MOF-derived metal nitrides/phosphides/chalcogenides have been synthesized and reported. In addition to the simplex MOF derivatives, the complex MOF derivatives with multiple properties often exhibited superior properties [118]. Song's group have reported an in-plane intergrowth CoS_2/MoS_2 ultrathin nanosheets [119]. In Fig. 8a, the CoS_2/MoS_2 nanosheets were obtained by one-step pyrolytic sulfurization of CoMo MOF precursors. The in-plane intergrowth structure of CoS_2 and MoS_2 generated rich contacted interfaces, and beneficial to optimize the electronic structures for enhanced catalytic behaviors. Apart from the preparation on heterogeneous sulfides, Schuhmann et al. have reported the preparation of hollow CeO_2@Co_2N nanosheets catalysts derived from Co-ZIF-L precursors by hydrothermal method and nitridation (Fig. 8b) [120]. The obtained CeO_2 @Co_2N catalysts exhibited rich phase boundaries, which promote the active CoOOH phase formation. The nitridation also add the numbers of accessible active sites, imply the huge potential of complex MOF derivatives. Li et al. developed a novel hybrid nanostructure with CoP nanoparticles (NPs) embedded in a N-doped carbon nanotube hollow polyhedron (NCNHP) derived from core-shell ZIF-8 @ZIF-67 for overall water splitting (Fig. 8e) [121]. The hollow polyhedron made of carbon nanotubes also remained and showed high porosity (Fig. 8 f). The HRTEM image of the CoP/NCNHP (Fig. 8 g) revealed fringe spacings of about 1.89 and 2.49 Å, corresponding to the (211) and (111) lattice planes of CoP, respectively. When the CoP/NCNHP was employed as both the anode and cathode for overall water splitting, it exhibited superior activity after continuously working with nearly negligible decay.

2.3.3. MOF-derived single-atom catalysts

Recently, single-atom catalysts (SACs) with single metal atoms anchored on the support materials have been a hot research spot. The SACs possess many advantages such as unique electronic structure, low-coordination surrounding, quantum size effect and robust metal-support interaction, endowing them superior catalytic performance in catalysis including electrochemical water splitting [122] However, it is different to engineer SACs with well-dispersed atomic active sites and favorable stability considering the agglomeration effect of SACs [123]. The

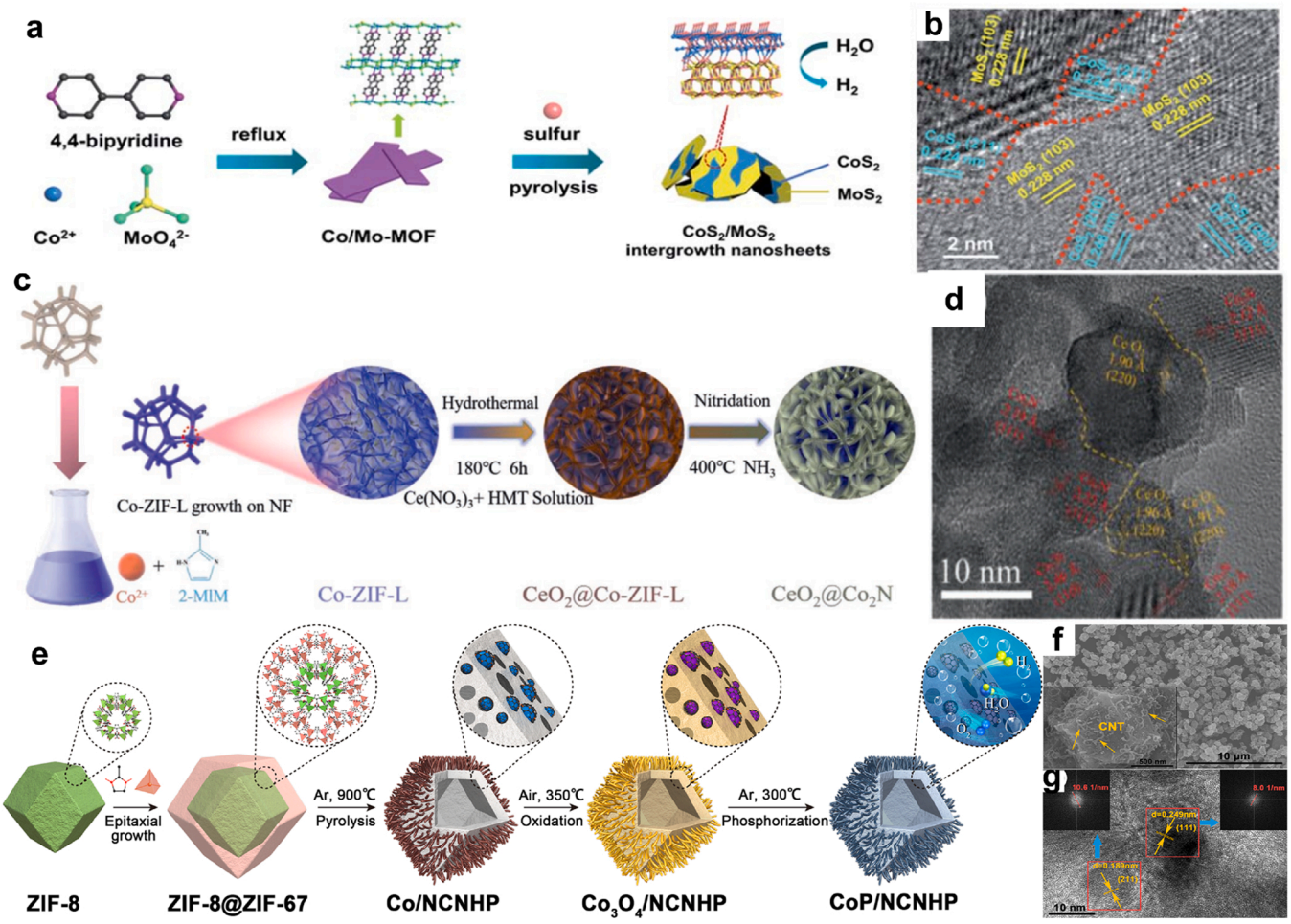

Fig. 8. (a) Schematic image of the in-plane intergrowth CoS_2/MoS_2 ultra-thin nanosheets, (b) HRTEM images of CoS_2/MoS_2 Nanosheets. (c) Schematic illustration of the synthesis of CeO_2@Co_2N. (d) HR-TEM images of CeO_2@Co_2N. (e) Schematic illustration of the synthesis process of CoP/NCNHP. (f) SEM and (g) TEM of the CoP/NCNHP catalyst. Inset in (f): magnified SEM image. Inset in (g): fast Fourier transformation of the selected area in the red box. (a-b) Reprinted with permission from Ref. [119]. Copyright (2020) Royal Society of Chemistry. (c-d) Reprinted with permission from Ref. [120]. Copyright (2021) American Chemical Society. (e-g) Reprinted with permission from Ref. [121]. Copyright (2018) American Chemical Society.

development of robust support materials that stabilize and activate SACs appear to be particularly important. The MOFs with ordered metal nodes and organic linkers have been confirmed as the advanced templates to support the SACs uniformly and efficiently [124]. Researchers have demonstrated that the SACs sites could be introduced to the metal nodes, ligands and pores in MOFs structures to construct, and undergo thermal pyrolysis or reduction to achieve the MOF-derived SACs catalysts [125]. The fascinating properties of MOFs also endows them with large surface area, benign pore architecture and adjustable catalytic properties, which play crucial role in catalytic reaction [126].

One typical example to synthesize the MOF-derived SACs is the controllable pyrolysis treatment. Wang's group have reported a kind of W atom catalyst support on MOF-derived N-doped C catalysts [127]. To be specific, the WCl_5 precursors were encapsulated in the skeleton of UiO-66-NH_2 by hydrothermal method. Then the high-temperature pyrolysis under 950 ℃ were operated to convert MOFs to zirconic oxides and N-doped C compounds. Finally, the HF was used to remove the zirconic oxide, the obtained MOF-derived W-SACs were synthesized. The pyrolysis strategy usually converts MOFs materials into robust N-doped C materials. However, the MOF-derived LDH could also act as support materials to anchor SACs. In Fig. 9a, Wu's group has designed a kind of amorphous/crystalline FeCoNi LDH supported Ru SACs catalysts (Ru SAs/AC-FeCoNi) [128]. Notably, Wu's group have designed a simple self-templating cation-exchange method to engineer this modified MOF-derived SACs that the LDH support could stabilize the Ru atoms well (Fig. 9b-c). It has also been verified that the single Ru atoms could lower the energy barriers to accelerate the catalytic reaction.

2.3.4. MOF-derived alloy catalysts

MOF-derived alloy materials have received significant attention for their unique characteristics for water splitting application [129]. Specially, MOFs can be used as precursors to synthesize alloy materials that exhibit high catalytic activity for water splitting. These MOF-derived alloy materials could combine the advantages of MOFs, such as high surface area and controllable composition, with the desirable properties of metal alloys, such as high conductivity and reactivity [130]. The resulting materials have shown great potential in improving the water splitting efficiency. These targeted materials have unique properties and high catalytic activity, making them become attractive candidates for use in industrial-scale water splitting systems [131]. Meanwhile, MOF-derived alloy materials are an important branch of MOFs derivatives for the applications in water splitting [132].

The metal atoms could be introduced and then alloy with other metals in the MOFs matrix to form the MOF-derived alloy catalysts. For example, the Pd-$CuCeO_x$ catalyst depicted in Fig. 9d involves a process wherein bimetallic MOF is synthesized as the precursor, followed by pyrolysis [133]. The step entails the formation of bimetallic CuCe-MOF with an organic ligand H_3BTC, with the introduction of Pd during the

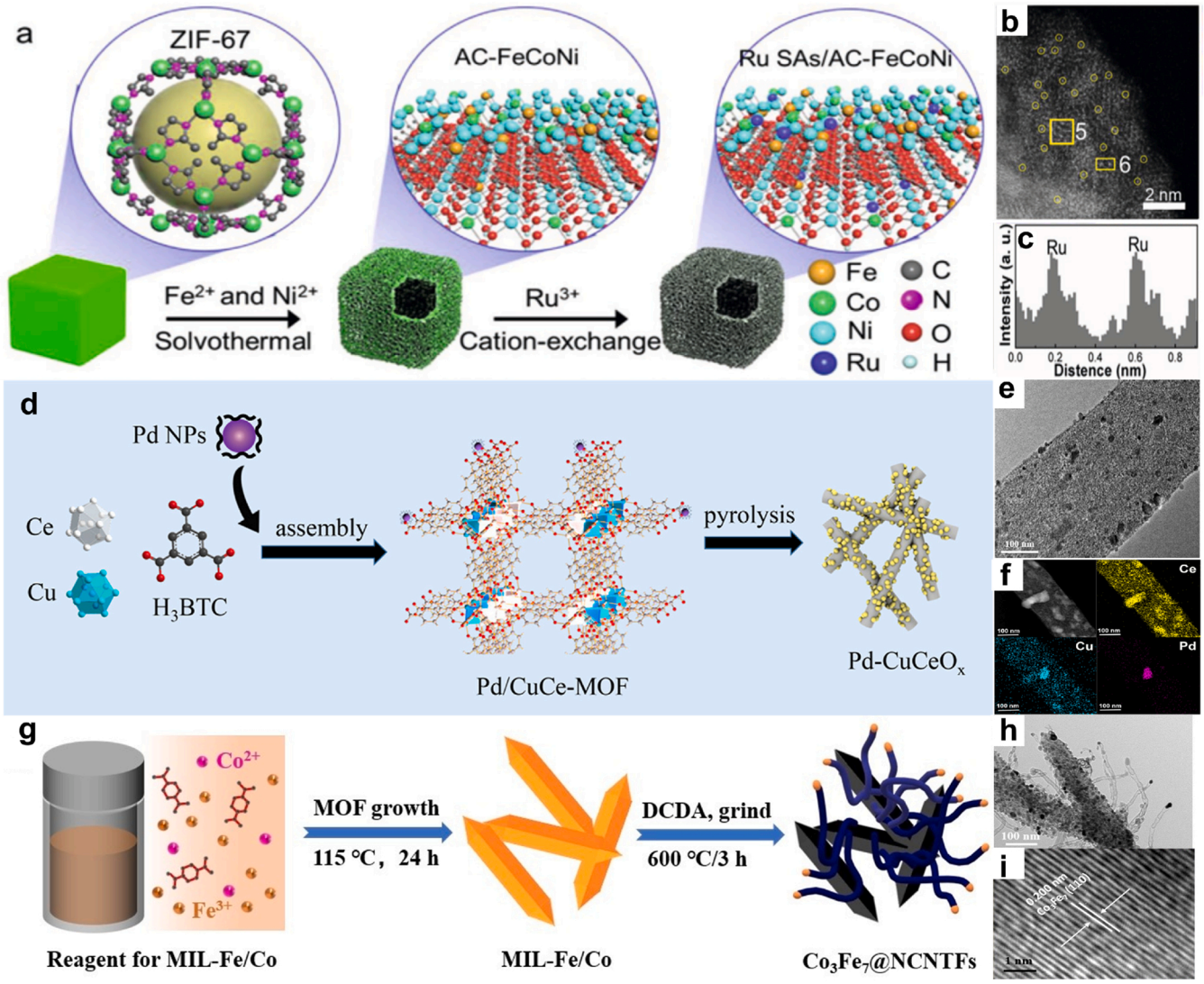

Fig. 9. (a) Illustration for the synthesis of Ru SAs/AC-FeCoNi. (b) AC HAADF-STEM image of Ru SAs/AC-FeCoNi. (c) Intensity profile along the middle of 6 from (b). (d) Synthesis process for bimetallic-MOF-derived Pd/$CuCe_x$. (e) TEM and (f) EDS elemental mapping of Ce, Cu and Pd, respectively of the Pd-$CuCe_x$ catalyst. (g) Schematic illustration of two-step synthesis of Co_3Fe_7 @NCNTFs. HRTEM images of (h) Co_3Fe_7@NCNTFs@NCNTFs and (i) the embedded of Co_3Fe_7 nanoalloy. (a-c) Reprinted with permission from Ref. [128]. Copyright (2021) Wiley-VCH. (d-f) Reprinted with permission from Ref. [133]. Copyright (2023) Elsevier. (g-i) Reprinted with permission from Ref. [134]. Copyright (2020) Wiley-VCH.

assembly process. The obtained bimetallic Pd/CuCe-MOF is pyrolyzed in an atmosphere of N_2. During this process, the Ce nodes in the MOFs react with oxygen in the organic ligand, resulting in the formation of CeO_2. Cu undergoes oxidation and is doped into CeO_2, while also alloying with the incorporated Pd. The Pd-$CuCeO_x$ catalyst consists of nanorods that are abundant in pores. The nanoparticles are evenly distributed throughout the nanorods and can be observed clearly (Fig. 9e). Moreover, EDS reveals the uniform distribution of Ce and Cu (Fig. 9 f). In addition, the MOF-derived alloy materials could be synthesized by in-situ chemical evolution without the foreign metal incorporation. The synthesis of Co_3Fe_7 @NCNTFs involved a typical two-step process, which is outlined in Fig. 9i [134]. The MIL-88-Fe/Co powder was mixed with dicyandiamide powder to form a uniform mixture, which was then pyrolyzed under vacuum at 600 °C for 3 h. TEM to confirm the structure of the carbon nanotube networks, which protruded from the rod-like morphology of the pyrolyzed frameworks (Fig. 9 h). The encapsulated nanoparticle possessed an interplanar distance of 0.200 nm, corresponding to the (110) lattice plane of Co_3Fe_7 nanoalloys (Fig. 9i).

3. Modified MOFs with high current density for water splitting

The US department of Energy has put forward a draft that the target current density should reach 3 A cm^{-2} at a cell potential of 1.9 V in a proton exchange membrane water electrolyzer (PEMWE) [135]. Therefore, developing high-current-density EWS catalysts is high desirable. The previous section has summed the classifications and robust engineering of modified MOFs, which have mostly become robust high-current-density OER/HER catalysts as well. Then, we would further conclude the key requirements for high current density, and inherent advantages with electronic structure tuning, defect construction and vacancy formation of these modified MOFs catalysts to realize large-current-density water splitting (Scheme 2).

The anodic OER and cathodic HER constitute the overall water splitting reaction. It is well-known that the catalytic performance of modified MOFs catalysts would be greatly influenced by the pH condition in both the OER and HER. (i) For pristine MOFs catalysts, rich metal sites and organic linkers in them could undergo the redox-active reaction under acidic/alkaline condition, which lead to the partial degradation of MOFs catalysts; (ii) For MOFs composites, different pH testing

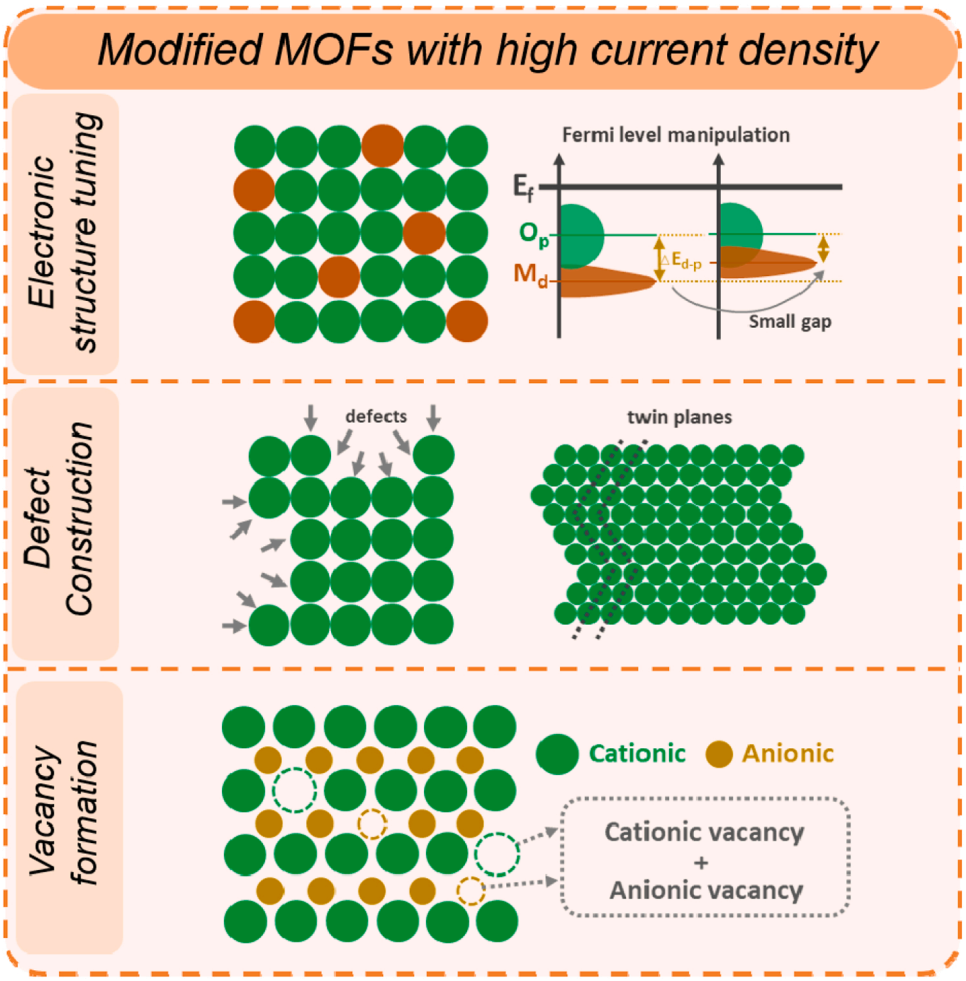

Scheme 2. Schematic illustration of modified MOFs with high current density.

media could not only result in the partial structural and compositional change, but also cause the possible evolution for other functional species such as the LDHs, metal alloys, and etc; (iii) For MOFs derivatives, on one hand, some MOFs derivatives are stable under the testing pH condition. On the other hand, some derivatives are not stable during the acidic/alkaline media, which could leach, dissolve, and even reconstruct. The evolution of MOFs catalysts under various pH condition would possibly transfer the surface metal sites into the real active species for promoted catalytic performance, however, the excess evolution could cause the degradation of modified MOFs materials as well, making them less stable over time.

Therefore, when designing and selecting MOFs and MOF-derived materials for water splitting, it is important to consider the pH conditions of the reaction environment, and to ensure that the materials have the appropriate activities and stability under those conditions. Herein, different kinds of modified MOFs catalysts under high-current-density operation for water splitting have been summed in Table 1.

3.1. Key requirements for high current density

Although most reported catalysts exhibit a low overpotential under the common 10 mA cm^{-2} for OER/HER. The activity and kinetic properties would largely affect under high current density (>200 mA cm^{-2}). The high current density EWS put higher requirements for catalysts referring to the active sites, electron transfer, and electrode stability [136,137].

For the active sites engineering, it has been confirmed that increase the amounts of active sites, improve the activity of a single active site and enlarge the exposure of active sites are rational approaches. In detail, the vacancy and defect are introduced to the MOFs catalysts motivate the activity of active sites [138] In addition, the rational tuning on electronic structures thus to promote electron distribution is beneficial for the improve the electron transfer ability, which facilitate the reactive kinetic enhancement [139]. Moreover, the drastic bubbles release could cause the exfoliation of electrode catalytic materials. More attention ought to be paid on the electrode stability needs to pay more attention. For that reason, the porous supports such as nickel foam (NF), carbon cloth (CC), carbon paper (CP) and other materials were adopted [140]. Their favorable mechanical strength and flexibility, good conductivity and large surface areas offer plentiful channels for mass and electron transfer, as well as bubbles release.

3.2. Electronic structure tuning

Most studies focus still focus on the superficial structure and morphology control, lacking the deep understanding of intrinsic electronic structures and leading to the limited performance improvement at a low over-potential. The electronic structure tuning is the most straightforward and efficient strategy to improve the activity of active sites, which refers to the regulation on occupancy of metal ions and e_g filling, mixed valency and d-band center, electron spin and distribution, and other microcosmic electronic properties. The rational control on the electronic structures is of great advantage for activate the activity of active sites for superior performances [141].

Generally, the redox-active *Oh* sites have a great impact on the catalytic behaviors of MOFs catalysts. The relationship between the e_g

Table 1
Summary of the characteristics of modified MOFs electrocatalysts for efficient water splitting.

Category	Modification	Catalysts	Performance under high-current-density operation	Ref.
Modified pristine MOFs	Trimetallic MOFs	$FeNiMn_{0.4}$-MIL-53/NF	OER: $\eta_{500\ mA\ cm^{-2}} = 290$ mV in 1 M KOH; 6.7% decay after 60 h	[66]
	NH_2-MIL-88B (Fe_2Ni) MOF on NF	NFN-MOF/NF	OER: $\eta_{250\ mA\ cm^{-2}} = 335$ mV in 1 M KOH; 7.8% decay @ 500 mA cm^{-2} after 30 h HER: $\eta_{250\ mA\ cm^{-2}} = 256$ mV in 1 M KOH	[67]
	FeCo-ONS as templates to form MOF-74 NSs	FeCo-MNS-1.0	OWS: 2.0 V @ 221 mA cm^{-2} in 1 M KOH	[68]
	Well-mixed and dispersed Fe- and Ni-MOFs	MFN-MOFs (2:1)/NF	OER: $\eta_{500\ mA\ cm^{-2}} = 294$ mV in 1 M KOH; 3.7% increase @ 500 mA cm^{-2} after 100 h HER: $\eta_{500\ mA\ cm^{-2}} = 234$ mV in 1 M KOH	[145]
	Ru-doped $Ni_2(BDC)_2TED$ MOF	NiRu-MOF/NF	HER: $\eta_{300\ mA\ cm^{-2}} = 209$ mV in 1 M KOH; slight increase @ 30 mA cm^{-2} after 24 h	[48]
	NiFe-BDC (X) SURMOFs (X = NH_2, H, OCH_3, and Br)	NiFe-MOFs	OER: $\eta_{200\ mA\ cm^{-2}} = 210$ mV in 0.1 M KOH	[49]
	Composition-balanced Fe, Co and Ni-based trimetallic MOFs	FCN-MOF	OER: $\eta_{500\ mA\ cm^{-2}} = 294$ mV in 1 M KOH; 5% decay @ 1000 mA cm^{-2} after 100 h	[61]
Modified MOFs Composites	Metal sulfide clusters embedded MOFs	NiFe-MS/MOF@NF	OER: $\eta_{300\ mA\ cm^{-2}} = 263$ mV in 1 M KOH; 11 mV increase over 17 h electrolysis HER: $\eta_{300\ mA\ cm^{-2}} = 234$ mV in 1 M KOH	[85]
	Conductive MOF/LDH heteronanotube arrays	cMOF/LDH	OER: $\eta_{300\ mA\ cm^{-2}} = 239$ mV in 1 M KOH; 7% decay @ 300 mA cm^{-2} after 24 h	[76]
	PPy and FeNi oxyhydroxides by polymerization on MIL-88	FeNi-PPy HNSs/NF	OER: $\eta_{200\ mA\ cm^{-2}} = 289$ mV in 1 M KOH; 20 mA cm^{-2} for 15 h	[69]
	Ultrathin NiO NPs within the 2D Ni-MOF	2D Ni-MOF-250	OER: $\eta_{1000\ mA\ cm^{-2}} = 239$ mV in 1 M KOH; 110 mA cm^{-2} after 20 h	[110]
	2D FeNi LDH packed with in-situ produced FeNi MOFs	2D/1D FeNi LDH/MOF	OER: $\eta_{276\ mA\ cm^{-2}} = 300$ mV in 1 M KOH; 7% loss @ 10 mA cm^{-2} after 36 h	[66]
	Metal hydroxide microarrays from MOFs	αCo$(OH)_2$-ZIF-L/NF-40	OER: $\eta_{500\ mA\ cm^{-2}} = 359$ mV in 0.1 M KOH	[79]
Modified MOFs derivatives	ZIF-67 derived cobalt phosphide	CoPO	OWS: 1.98 V @ 200 mA cm^{-2} in 1 M KOH	[89]
	Phosphorization on CoFe MOF TPAS/Ni	CoFeP	OER: $\eta_{700\ mA\ cm^{-2}} = 335$ mV in 1 M KOH; 15 mV potential change after 100 h HER: $\eta_{900\ mA\ cm^{-2}} = 263$ mV in 1 M KOH; 10 mV potential change after 100 h	[92]
	Sulfur-treated Fe-based MOFs	Fe_{MOF}-SO_3	OER: $\eta_{500\ mA\ cm^{-2}} = 298$ mV in 1 M KOH; 3% decay @ 1000 mA cm^{-2} after 100 h	[88]
	F-doped CoFe phosphides	F-Co_2P/Fe_2P/NF	HER: $\eta_{2000\ mA\ cm^{-2}} = 292.2$ mV in 1 M KOH; 2000 mA cm^{-2} for 10 h	[97]
	Etching ZIF-67, PBA formation and phosphating in turn	NC@FeP_4-CoP	OWS: 1.72/1.80 V@ 500/1000 mA cm^{-2} in 1 M KOH, 500 mA cm^{-2} for 48 h	[137]
	Sn-RuO2 NPs on MOF-derived N-doped C polyhedra	$Sn_{0.1}$-RuO_2 @NCP	OER: $\eta_{200\ mA\ cm^{-2}} = 290$ mV in 0.5 M H_2SO_4; 42 mV change @ 10 mA cm^{-2} after 150 h	[94]
	Ultralow Ru doping amorphous Co-based oxide	Ru-CoO_x/NF	OER: $\eta_{1000\ mA\ cm^{-2}} = 370$ mV in 1 M KOH; 80 mA cm^{-2} for 100 h HER: $\eta_{1000\ mA\ cm^{-2}} = 252$ mV in 1 M KOH; 70 mA cm^{-2} for 100 h	[99]

occupancy in the *Oh* sites and the OER activity obey the volcano trend, which indicated that the rational control on the *Oh* occupied metal ions could improve the OER performance [142]. Herein, it is crucial to adjust the e_g orbitals in metal centers and O 2p orbitals in oxygen species to achieve the optimal overlap. In addition, the formation of O-O bond needs the participation of high-valence metal states. The mixed valency introduction is beneficial to boost to O-O bond generation with maximum interacted with reaction adsorbates [143] Meanwhile, the well-tuned d-band center could adjust the adsorption energy of different oxygen intermediates. Apart from the e_g filling and d-band regulation, other electronic structures such as electron spin states, distributions could also be engineered to optimize the catalytic activity [144].

For overcoming the aimless experiential exploration on the relation between electronic structure and catalytic activity, Jiang's group have deigned an integrated theoretical-experimental approach for discovering the quantitative connection between electronic structure and OER activity [145]. Therefore, a class of Ni-M-MOFs (M=Fe, Co, Cu, Mn, and Zn) were obtained. The DFT calculations referring to the electronic structures involving d-band center (E_d) and projected density of states (PDOS) for 3d e_g filling (f_e) orbitals were conducted to investigate the M-replacement effect on the Ni-MOF electronic structure (Fig. 10a). It has been confirmed that the filled bonding states and partial occupied antibonding states were formed by a coupling between *d* orbits in metals and *p* orbits in oxygen species. The E_d and f_e were crucial parameters for describing the OER activity in terms of electronic structures. Moreover, the E_d variation often accompanied by the f_e change in the Ni-M-MOFs. In Fig. 10b, the E_d and f_e of different catalysts exhibits a linear relationship, implying the similar mechanism in optimizing the OER activity as calculated (Fig. 10c). The calculation on E_d and f_e could not only tune the electronic structures of different catalysts for enhanced activity, but also serve as useful descriptors to predict the OER activity. As a result, the optimized NiFe-MOF achieved a superior OER activity with a low overpotential of 278 mV at a high current density of 250 mA cm^{-2} (Fig. 10d and e), which is 188 mV less than that of Ni-MOF. The NiFe-MOF also exhibited the favorable reactive kinetics performance (Fig. 9 f). The quantitative electronic structures tuning in Ni-M-MOFs endows them with superior activity in high-current-density OER process.

Apart from the E_d and f_e tuning, the regulation on electronic spin state and orbital interaction has also been proven as efficient strategies to improve the catalytic activity. A typical example is the spin-sate reconfiguration by altering the magnetic field for boosting the OER. Liu's group have designed a magnetic-stimulation method to control the spin electron distribution in CoMn MOFs (Fig. 10 g and h) [146] As a result, Liu's group have revealed the role of the spin-dependent reaction pathway. The local magnetic heating leads to the spin flip at certain active sites, contributing the spin-dependent activity. The spin-optimized $Co_{0.8}Mn_{0.2}$ MOFs exhibited a lower overpotential under large current density. In addition to the E_d and f_e tuning and spin-state regulation, the electronic structures engineering on binding energy of intermediations and valence of metal ions have been reported. Lee et al. have reported a binding energy tuning on H intermediates to activate the inert Cu atoms for boosting the HER activity by ultralow Ru doping [147] The DFT calculations demonstrated the optimized H* binding energy, which endows Ru-Cu-3 catalysts superior HER activity to rival Pt/C. In addition, Zhu et al. have proposed a self-optimized OER activities by the gradual Fe valence increasement [148]. The FeNi MOFs exhibited a low overpotentials of 308 mV at a large current density of

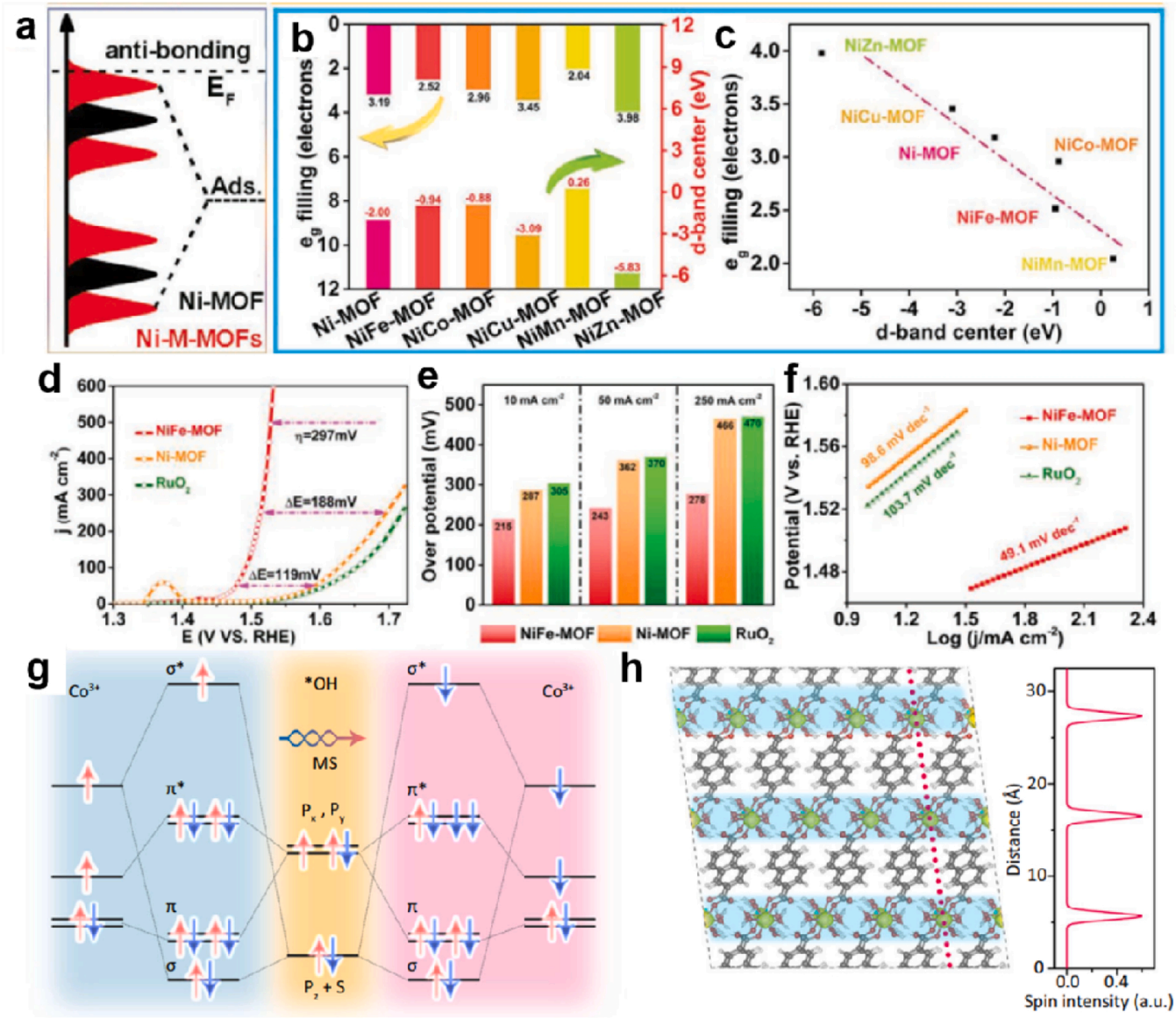

Fig. 10. (a) Schematic illustration of bond formation between the catalyst and the adsorbate (Ads.),(b) corresponding values and (c) correlation between the d-band center and eg filling for substituted M in Ni-M-MOFs, (d) LSV curves of the catalysts, (e) overpotential required for j = 10, 50, and 250mA cm^{-2}, (f) Tafel plots, (g) the orbital interaction between Co and *OH and (h) the spin density distribution of $Co_{0.8}Mn_{0.2}$-MOF. (a-f) Reprinted with permission from Ref. [145]. Copyright (2021) Wiley-VCH. (g and h) Reprinted with permission from Ref. [146]. Copyright (2021) NaturePublishing Group.

200 mA cm^{-2}, suggesting effective electronic transfer by the role of Fe-O bond covalency.

3.3. Defect construction

The defects are often generated in the synthesis catalytic materials. It is of great importance to understand the introduction of defects and thus to design high-efficient catalysts. To be sure, the point defect often considered as vacancy, which would be clarified in next section. In addition, there are still many kinds of defects, including lattice defects (dislocation, step, and etc), plane defects (grain boundary, stacking dislocation and etc) and structure defects [149]. The distinct linker defect should also be considered in MOFs catalysts. Meanwhile, many efficient defect introduction strategies have been developed, including atom doping, thermal treatment, chemical reduction, etching, strain inducing, and etc [150]. The rational control on the defect construction could adjust the local atomic structure and add reactive active sites for catalytic activity enhancement, which also help catalysts achieve higher current density for water splitting [151].

Lee's group has developed a kind of defective MOF-derived RuO_2 nanosheets by heat treatment [152]. As shown in Fig. 11a, the prepared RuO_2-NS/CF possess abbundant lattice defects in the crystal structures, indicating the favorable instrinsic activity. As a result, the LSV curves demonstrated that the RuO_2-NS/CF catalysts exhibited lower overpotential at 10 and 200 mA cm^{-2} than other catalysts (Fig. 11b). In addition to the lattice defects. The linker defects in MOFs catalysts were induced to add the active sites for enhanced activity. Li's group has engineered a missing linkers CoBDC-Fc-NF catalysts with rich defect sites [46]. As shown in Fig. 11c and d, the perpared CoBDC-Fc-NF catalysts exhibited the sperior catalytic properties with a low overpotential of 267 mA cm^{-2} at a high current density of 500 mA cm^{-2}. Moreover, Liu et al. have reported a defective MOFs with open Lewis acidic sites and missing linker defects by ligand exchange strategy [153]. This defect inducement benefits to generated MOFs with adjustable short-range disorder/long-range order structure for heterogeneous phase construction. The prepared Co@CoO catalysts showed favorable

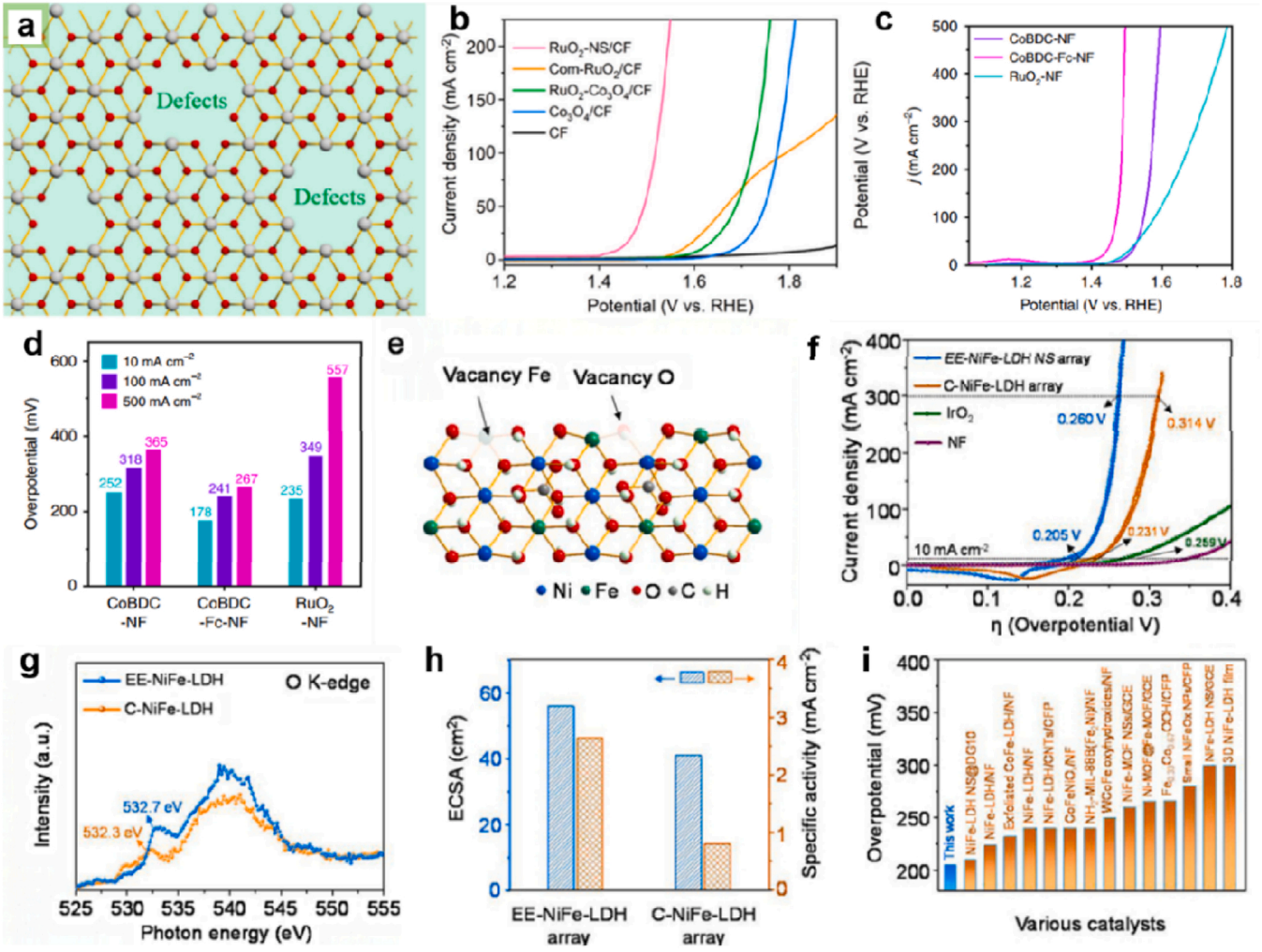

Fig. 11. (a) Atomic model of the RuO_2-NS/CF structure, (b) LSV curves of different catalysts, (c) LSV curves and (d) mass activity of CoBDC-Fc-NF, CoBDC-Fc-NF and RuO_2-NF catalysts, (e) atomic structure illustration of EE-NiFe-LDH with Fe and O vacancy, (f) CV/LSV plots of tested catalysts, (g) O K-edges XAS spectra and (h) ECSA and ECSA-normalized specific activities of EE-NiFe-LDH and C-NiFe-LDH, and (i) comparison of η @ j = 10 mA cm^{-2} of various catalysts. (a and b) Reprinted with permission from Ref. [152]. Copyright (2021) Elsevier. (c and d) Reprinted with permission from Ref. [46]. Copyright (2019) Nature Publishing Group. (e-i) Reprinted with permission from Ref. [160]. Copyright (2021) Elsevier.

HER activity.

3.4. Vacancy formation

The vacancies are the simplest defects in nanomaterials, which usually known as point defects referring to the absence of atoms at the lattice sites [154]. The vacancy could be introduced by many synthetic methods, such as calcination, chemical reduction, ion doping, plasma etching, and etc [155]. Generally, the vacancy density could also be tailored by controllable introduction condition. MOFs catalysts are composed by different metal atoms and non-metal atoms, which could form vacancies in wide diversity [156]. Notably, the vacancy families were constituted by anion vacancy, cation vacancy, and multi vacancy [157]. These different vacancies have been demonstrated to significantly improve the water electrolysis efficiency. To be specific, the oxygen vacancy (V_O) is the most famous anion vacancy in MOFs catalysts, which exhibited the reducibility of M-O bond and low hopping barriers [158]. The V_O-rich MOFs catalysts with more exposure active sites are also demonstrated to possess enhanced catalytic activity. Apart from the common V_O, some researchers reported the cation vacancies for optimizing the catalytic behaviors in MOFs catalysts [159].

Recently, in addition to the single vacancy, the prepared MOFs catalysts also show multi vacancies (both cation and anion defects), the co-existing vacancies within one system would function in a synergistic way to accelerate the catalytic reactions, which served as novel and efficient method to boost high-current-density water splitting. For example, Liu's group have engineered a structure inheritance strategy to fabricate the MOF-derived EE-NiFe-LDH catalysts [160]. In Fig. 11e, the obtained catalysts possess both cation vacancy (Vacancy O, V_O) and anion vacancy (Vacancy Fe, V_{Fe}). The co-existing of V_O and V_{Fe} contributed to a superior catalytic activity, which deliver a low overpotential of 260 mV at a high current density of 300 mA cm^{-2}, indicating the robust synergistic role of multi vacancy (Fig. 11 f). To further investigate the activity origin, O K-edges XAS spectra of catalysts were analyzed (Fig. 11 g). The positive shift of O K-edge peak implied the increased V_O density. Benefitting from the vacancy-rich structure, the EE-NiFe-LDH catalysts exhibited larger electrocatalytic surface areas than the C-NiFe-LDH catalysts (Fig. 11 h). Moreover, the catalytic behavior of EE-NiFe-LDH also exceeded many other reported catalysts (Fig. 11i).

4. Modified MOFs with long-term stability for water splitting

The reported catalysts were mostly tested on a common low current density (10 mA cm^{-2}) for several hours (<100 h). However, the US Department of Energy has set a goal of more than 80000 h working time

for PEMWE by 2025. The catalytic performance of existing catalysts is far from the requirement [161]. Generally, the catalytic durability was greatly influenced by the leaching and loss of catalysts under acid/-alkaline condition, as well as the exfoliation from the electrodes owing to the violent bubble generation [162]. Under the circumstances, it is important to enhance the structural stability and mechanical sturdiness. Researchers have developed many well-modified MOFs catalysts, we thereby concluded the key requirements for long-term stability and discussed the merits of those modified MOFs catalysts to realize long-term durability water splitting (Scheme 3).

4.1. Key requirements for long-term stability

As discussed above, the MOFs catalysts tend to suffer the leaching and exfoliation by testing conditions and bubbles impact. It is of great significance to develop catalysts with superior long-term durability, which just change 10% of current density after more than 100 h tests. Hence, the high demand of long-term stability put higher requirements for catalytic stability including structural stability and mechanical sturdiness.

Both the stabilities are important to the whole durability improvement in water splitting. For one thing, the structural stability involves the anti-corrosion and anti-leaching abilities, which require that the active species in catalysts could stable in the acid/alkaline conditions [163]. For another, the mechanical sturdiness refers to the ability to resist the impact force oriented from the generation and diffusion of continuous bobbles (O_2 or H_2). Herein, the interaction between catalysts and support should be reinforced [164]. Finally, the structural reconstruction phenomenon usually occurred on the catalytic surface and interface [165]. On one hand, the negative structural reconstruction could lead to the loss and evolution of active species; on the other hand, the positive one could contribute the continuous exposure of active centers, or convert surficial catalysts into more active species [166]. The efficient structural reconstruction should also be rationally utilized to improve the long-term stability.

In this section, we mainly discussed the three strategies in modified MOFs catalysts including active sites protection, catalytic support reinforcement and efficient surface structure reconstruction to largely improve the catalytic long-term stability. Most studied adopted CP and CA tests to evaluate the catalytic stability. We additionally discussed the in-situ characterization to uncover the activity origins and dynamic evolution of active sites.

4.2. Active sites protection

It has been confirmed that the active sites in MOFs catalysts were composed of metal species. The metal species served as active centers are susceptible to suffer oxidation, dissolution, leaching and evolution in acid/alkaline electrolyte during the reaction time, resulting in the unfavorable catalytic behaviors [167]. Therefore, protecting the active sites thus to prevent negative activity loss is highly desirable. Researchers have also developed efficient approaches to protect the active sites [168–170].

One efficient strategy is the introduction of high-valence metals, which could optimize the adsorption energy of intermediates and prevent the over-oxidation of active species thus to improve the catalytic

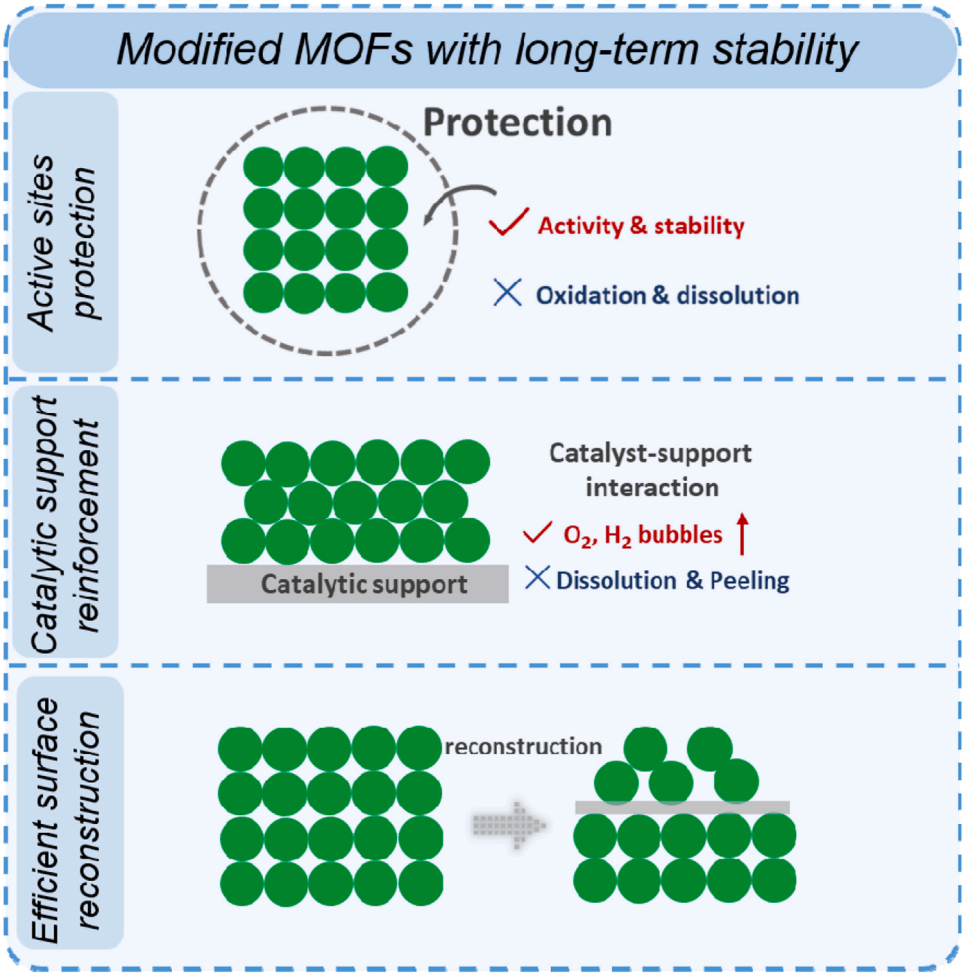

Scheme 3. Schematic illustration of modified MOFs with long-term stability.

activity. For example, Fransaer's group have obtained a kind of hierarchical MOF-derived Ni_3S_4 catalysts [171]. The Ni_3S_4 catalysts exhibited long-term stability at 50 mA cm^{-2} for 300 h with no degradation for OER (Fig. 12a). The high-valence Ni^{3+} could enhance the chemisorption of OH^- to prevent the coverage of active sites, which facilitates the electronic transfer and increase the active sites for stable and continuous OER. Another strategy is the formation and introduction of amorphous phase. Li's group have designed a kind of MOF-derived FeOOH/CeO_2 heterolayer nanotube catalysts (Fig. 12b) [172]. The formed FeOOH layer could inhibit the mass loss of Ce species and provide strong electron interaction platform for superior electronic/ionic conductivity. As shown in Fig. 12c, the FeOOH/CeO_2 catalysts could achieve the highest current density at 300 mV among the tested catalysts. Moreover, the CP experiments conducted at different overpotentials including 250, 300, 350 and 400 mV for 50 h demonstrated the superior stability of catalysts (Fig. 12d).

4.3. Catalytic support reinforcement

It has been reported that the catalysts loading on the support and the catalysts-support interaction have great impact on the catalytic stability. For one thing, excess loading on electrode would lead to the falling and exfoliation of catalytic materials and thus affect the stability [173]. For another, low mass loading on the electrodes tend to exhibit limit catalytic active sites, which makes it difficult to maintain the high-current-density water splitting for a long time [174]. Hence, it is necessary to optimize the loading amount on the electrodes for maximized catalytic stability.

In addition, strengthening the catalyst-support interaction is another strategy to enhance long-term stability. The robust supports such as nickel foam (NF), carbon cloth (CC), carbon paper, and etc have been used to support the catalysts. For instance, the NF could improve the electron transfer efficiency and facilitate the active center exposure. The unique substrate structure could eliminate the generated bubbles to avoid the unnecessary accumulation on the active sites, which provide a stable platform to proceed the high-current-density for a long period [175,176]. Apart from the NF, CC substrate, the in-situ formed LDHs could also strengthen the interaction with catalytic support. In Fig. 12e-g, Zhai's group have reported a lattice-matching growth strategy to prepare a kind of conductive MOF/LDH catalysts on CC for efficient water splitting [65]. The CoNiFe LDH could serve as interior template to construct an interface by inlaying cMOF and matching two crystal lattice systems. In addition, the multi-current step CP response of cMOF/LDH-48 catalysts were operated to display the shorted diffusion paths for OH^- charge carriers and fast gas bubble dissipation. The obtained catalysts on CC supports exhibited the superior catalytic stability with no obvious decay (Fig. 12 h). The CC support could provide a hydrophilic surface to support the growth of LDH, which strengthen the

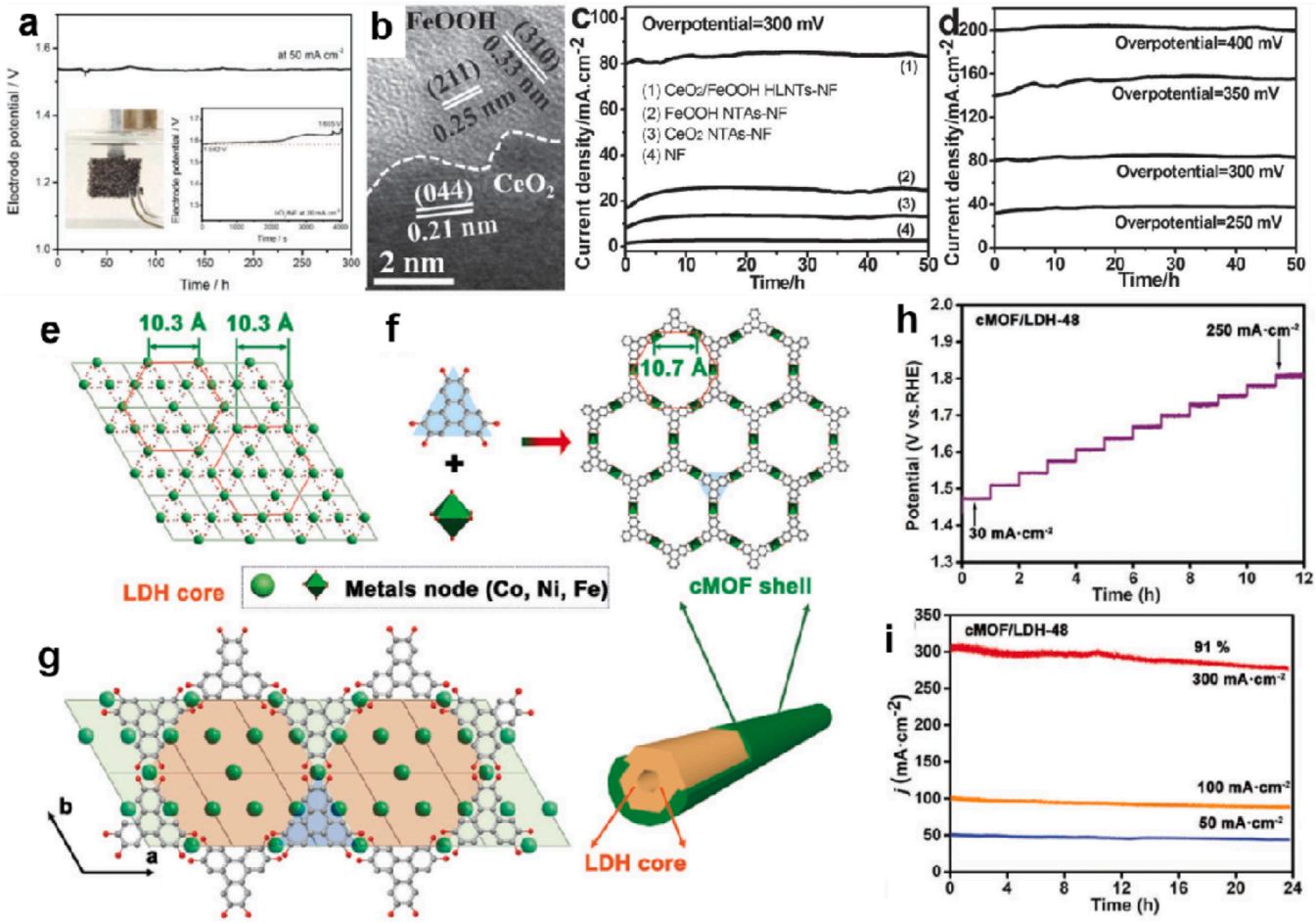

Fig. 12. (a) Full water splitting at 20 mA cm^{-2} in 1.0 M KOH (inset a photograph during water splitting), (b) HRTEM image of FeOOH/CeO_2, (c) CP tests of long-term stability of tested catalysts for 50 h at the overpotential of 300 mV, (d) long-term stability tests of FeOOH/CeO_2 HLNTs-NF for 50 h, (e) (002) crystal plane of CoNiFe-LDH, (f) (001) crystal plane of cMOF, (g) grafting growth of (001) crystal plane from cMOF onto (002) crystal plane from CoNiFe-LDH, (h) multi-step CP curve of cMOF/LDH-48 with current densities increasing from 30 to 250 mA cm^{-2}, (i) stability tests of cMOF/LDH-48 with different current densities. (a) Reprinted with permission from Ref. [171]. Copyright (2019) Wiley-VCH. (b-d) Reprinted with permission from Ref. [172]. Copyright (2016) Wiley-VCH. (e-i) Reprinted with permission from Ref. [65]. Copyright (2022) Wiley-VCH.

interaction between each other. The prepared catalysts also exhibit < 10% activity loss after high-current-density stability tests (300 mA cm^{-2}), indicating the synergistic role of catalytic supports.

4.4. Efficient surface reconstruction

The surface reconstruction refers to the evolutions on surface properties of catalysts during catalytic process such as HER and OER, mainly oriented from the external environment changes including applied voltage and test electrolytes [177]. Generally, if the operating voltage is higher than the redox potential of elements in catalysts, the roughness, porosity, composition, chemical valence, crystal plane and crystallinity would change, and thus lead to the topological, chemical, and crystallographic reconstruction of surface layer [178,179]. Meanwhile, the test electrolyte would also act as the medium to influence the reconstruction process.

It has been reported that the in-situ formed surface layer could continuously serve as the active sites for improving the catalytic stability. For example, the active species would form when the modified MOFs catalysts served as catalysts, hence the catalytic composition and behaviors would be changed by the reconstruction. Lin's group have reported a kind of MOF-derived Cr-NiS_2/C@NF catalysts with self-reconstruction for long-term OER [180]. In Fig. 13e, the voltage-dependent self-reconstruction revealed that the $Ni(OH)_2$ species would firstly formed, and convert to NiOOH species reversibly according to the high/low voltage change. As a result, the NiOOH as newly-formed active species possessed high OER activity and promote the long-term stability with no negative effect, which endowed Cr-NiS_2/C@NF catalysts with favorable stability for 80 h at 30 mA cm^{-2} (Fig. 13f). Other study also investigated the dynamic equilibrium for updated reconstructed surface layer. For instance, Dong et al. have reported a series of FeOOH-Ni-based catalysts for establishing the catalytic equilibrium [181]. In Fig. 13a-c, the introduction of tiny Fe^{3+} would maintain the stability well by reducing the oxidation potential. Correspondingly, the relative LSV curves displayed the similar tendency. It could be concluded that catalytic interfaces were damaged owing to the Fe species loss during the long-stability tests while Fe^{3+} species tend to transform into FeOOH species. Herein, the addition of Fe^{3+} species would facilitate the establishment of catalytic equilibrium interface. It has been verified that the continuous introduction of Fe^{3+} species could maintain the high-current-density OER with superior long-term durability. The stability of FeOOH-NiBDC-NF catalysts was not only no loss, but also improve to a certain extent due to the dynamic equilibrium reconstructed FeOOH species.

We have focus on the regulation methods for the enhancement on high current density activity and long-term stability, respectively. The strategies with electronic structure tuning, defect construction and vacancy formation were adopted in modified MOFs for the activity improvements. Correspondingly, the strategies with the active site protection, catalytic support reinforcement, efficient surface reconstruction were employed to promote the long-term stability. (i) The active site protection method mainly referred to the introduction of high-valance metal and hydroxyl oxides to protect the metal active species which suffered from the oxidation, dissolution and leaching; (ii) The catalytic support reinforcement strategy referred to the adoption on the support materials such as nickel foam (NF), carbon cloth (CC), carbon paper, and etc to promote the bobbles releasement during OER/HER process to avoid the shedding and stripping of catalysts; (iii) The efficient surface reconstruction method referred to the reconstruction reaction to obtain the newly-formed active sites such as metal hydroxyl oxides to maintain the long-time electrocatalytic reaction for improved stability.

In general, we have concluded the strategies on the stability enhancement referring to the active sites protection, catalytic support reinforcement and surface reconstruction considering the changes of catalysts during the electrochemical water splitting catalysis. However,

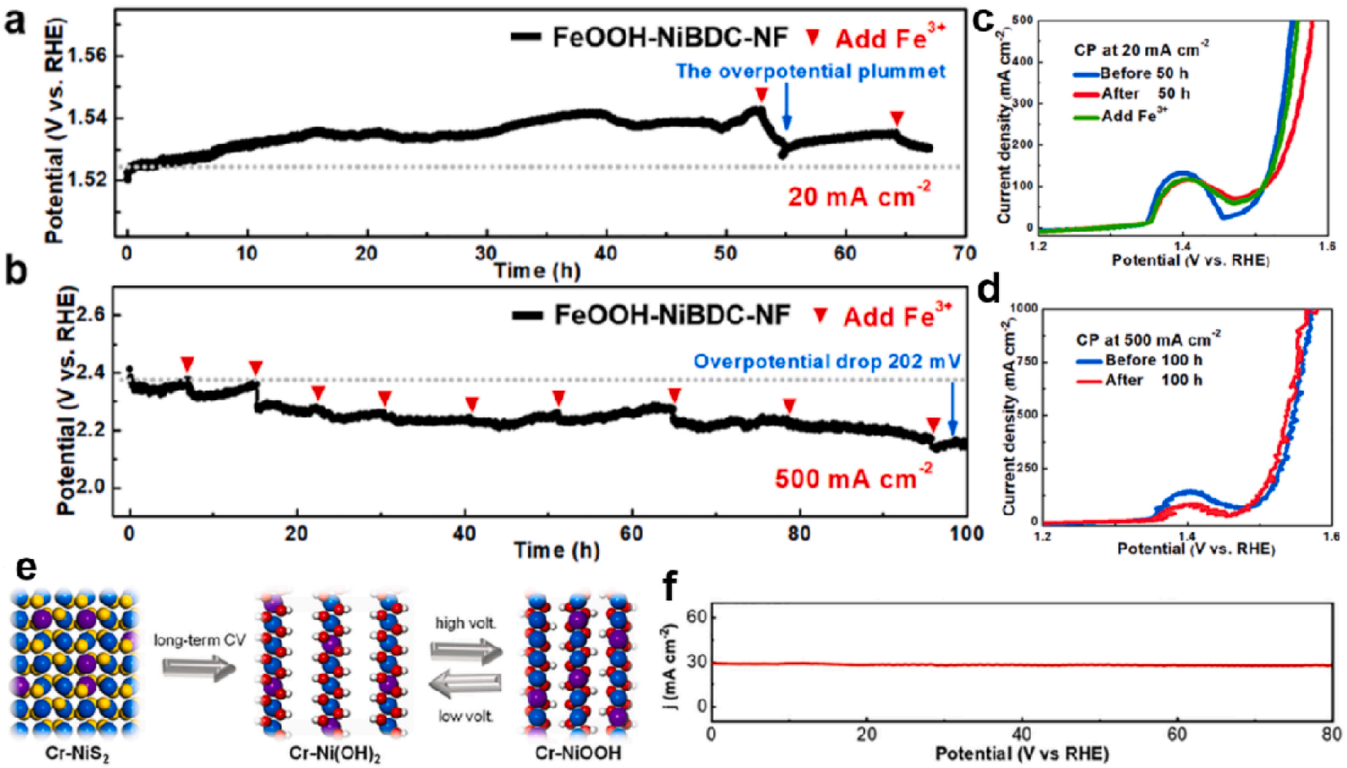

Fig. 13. (a) The CP test of FeOOH-NiBDC-NF at 20 mA cm^{-2} and b) 500 mA cm^{-2}, (c) LSV curves of FeOOH-NiBDC-NF before and after CP test at 20 mA cm^{-2} and (d) 500 mA cm^{-2}, (e) illustration of the self-reconstruction during CV cycling, and (f) i-t curve of Cr-NiS_2/C@NF in OER at an overpotential of 245 mV. (a-d) Reprinted with permission from Ref. [180]. Copyright (2022) Elsevier. (e and f) Reprinted with permission from Ref. [65]. Copyright (2022) Elsevier.

the practical water splitting often face more complexed and demanding conditions, especially under large current density. Basically, a higher bias would applied to the modified MOFs catalysts, which would lead to a more extreme polarization condition far from the equilibrium potential. In addition, the violent and fast electrocatalytic reactions caused more fast consumption on the reactants and fast generation of products.

These differences cause catalytic stability under large current density different to that under low current density, which were as follows: (i) faster and intensive electron transfer at catalyst-electrolyte and catalyst-support interfaces; (ii) massive mass transfer at the gas-liquid-solid interface referring to the reactants, products, and catalysts; (iii) robust mechanical and chemical stability; (iv) strict requirement on practical proton exchange membrane water electrolyzers (PEMWEs) and alkaline anion exchange membrane water electrolyzers (AAEMWEs). Although the above-mentioned strategies with active sites protection, catalytic support reinforcement and surface reconstruction have been adopted to improve the electrochemical water splitting stability. Other important factors also should be considered based on these differences: (1) well-optimized electron transfer interaction. It has been confirmed that constructing large specific areas and efficient hierarchical structures could help to boost the charge transfer and resist the morphological collapse and compositional loss. (2) development on more kinds of catalytic supports materials. Apart from the previously-reported nickel foam and carbon cloth supports, more advanced supports such as iron foams, Mxenes, and even covalent organic frameworks have been adopted to serve as catalytic supports. (3) practical tests on PEMWEs or AAEMWEs. Considering that the catalytic stability of most modified MOFs materials was measured under the laboratory condition, the local environment near the surface of OER catalysts tends to be more acidic than bulk electrolytze in the PEMWEs and more alkaline in AAEMWEs. Herein, the true electrochemical durability on the practical devices is highly desirable.

5. Conclusions and outlook

In this review, we firstly concluded the classifications of modified MOFs, including the modified pristine MOFs with metal node engineering and ligand regulation, modified MOFs composites with MOFs@MOFs, LDH/MOFs, cluster/nanoparticles@MOF, conductive polymer@MOF and COF@MOF, modified MOFs derivatives with MOF-derived oxides and oxyhydroxides, nitrides/phosphides/chalcogenides and MOF-derived single-atom catalysts. Those modified MOFs catalysts show huge potential for the high-current-density and long-term stability for water splitting. Generally, strategies are developed in MOFs catalysts to boost the activity such as electronic structure tuning, defect construction and vacancy formation. Meanwhile, the approaches such as active sites protection, catalytic support reinforcement and efficient surface reconstruction were also developed to enhance the stability. However, it is still remains a great challenge of these modified MOFs catalysts for the industrialized application such as PEMWEs, mainly referring to the following four aspects (Scheme 4).

i) *Efficient modified MOFs catalysts construction:* Although many modified MOFs catalysts have been reported, which is still far from the industrial demand. Firstly, the synthesis mainly focuses on the trial and error based on empirical disciplines, lacing the universal and large-scale synthesis. Secondly, the inherent merits such as high porosity and high surface areas would be damaged to some extent after certain treatments, which makes it difficult to design efficient modified MOFs with those advantages. Finally, the poor conductivity of MOFs catalysts is always the key point to improve, while some conductive MOF materials have been developed. It is highly desirable to engineer robust catalysts based on efficient conductive pristine MOFs materials under the theoretical design and even machine learning.

ii) *Deep insight in active sites:* The modified MOFs electrocatalysts are often composed of multi-metal compounds. Meanwhile, the surface structure would also reconstruct after OER and HER process, which makes it difficult to determine true active sites. It is crucial to accurately determine and directly observe the active centers evolution. Several advanced characterization techniques have been developed and applied to the characterization of MOF-modified results. Therefore, the in-situ technology such as in-situ FTIR, in-situ Raman, in-situ TEM, in-situ XRD, and other techniques had been developed. The in-situ characterizations also realize the visualization by monitoring the operation conditions, structural changes, phase transitions, and species formation during OER and HER process. In addition, the extended X-ray absorption fine structure (EXAFS) and X-ray absorption near-edge structure (XANES) spectra based on the synchrotron radiation techniques were developed to the analyze the electronic state and atomic configuration to confine the real catalytic center. Furthermore, the isotopic tracing method is another robust strategy to reveal the reaction path and catalytic sites. In summary, these techniques provide important insights into the structure, morphology, chemical and electronic properties, and dynamic behavior of MOFs, and can aid in the optimization of their performance in water splitting.

iii) *High current density and long-term durability:* The further development of advanced catalysts with high-current-density and

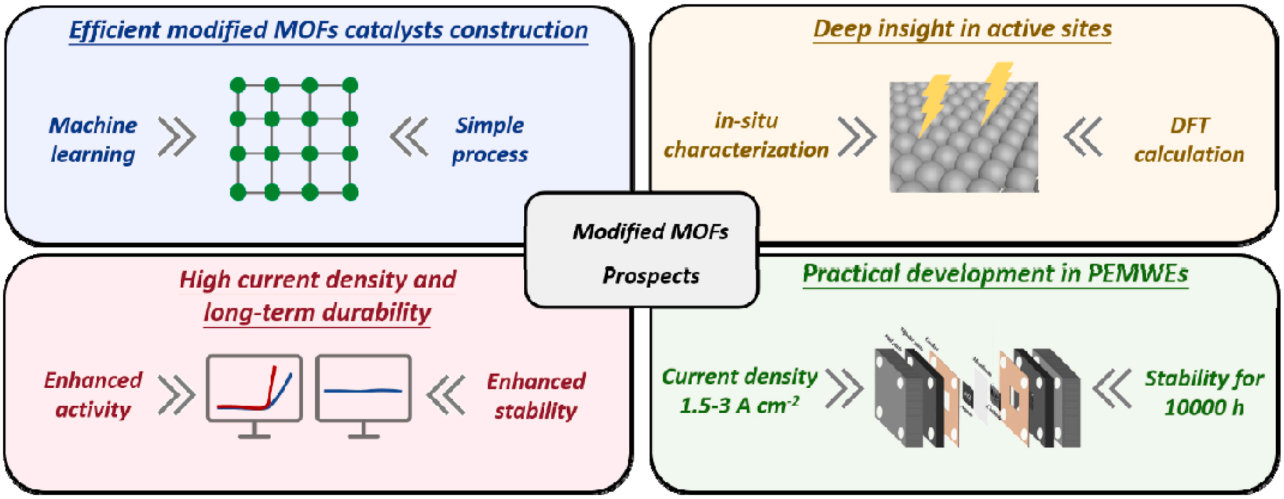

Scheme 4. Perspectives of modified MOFs under high current density operation and long-term stability.

long-term stability to meet the industrial demand is of great importance. Generally, the crucial factors in the performance enhancements lie in the promotion on intrinsic activity and the long-time structural and mechanical stability, which corresponding to the existing evaluation parameters such as the current density at 10 mA cm^{-2} and stability with dozens of hours. However, those parameters are not applicable in the the further water electrolysis progress. Herein, the new evaluation indictors including overpotential at 200 mA cm^{-2}, stability with thousands of hours, recoverability and etc should be considered and exploited in measuring the high-current-density water splitting [182].

iv) *Practical development in PEMWEs:* The practical development in PEMWEs is the final goal for designing efficient catalysts with large current density and long-term stability, same for the modification on MOFs catalysts. At present, some high-performance modified MOFs catalysts have been developed to apply in PEMWEs [183]. In addition, the US department of energy proposed other key standards based on the manufacturing costs and large-scale production, involving the low/high temperature electrolysis for hundreds of thousands of hours, efficiency, and others. As the mentioned above, a small part of prepared MOF-derived catalysts had been reported as the potential catalytic materials in PEMWEs or AAEMWEs. However, we could synthesize the promising industrial MOF-based catalysts only by trial and error based on the current studies. Meanwhile, this review emphasized the optimized strategies with better catalytic performance, which set the further practical applications as the final goal. The modified MOFs catalysts still have a long way to go towards the wide application of high-current-density PEMWEs.

Declaration of Competing Interest

The authors declare that they have no known competing financial interests or personal relationships that could have appeared to influence the work reported in this paper.

Data Availability

No data was used for the research described in the article.

Acknowledgements

This work is supported by the start-up funding to F. Gao by Jiangsu University of Science and Technology (1112932206) and National Natural Science Foundation of China (Grant No. 52073199, 51873136, 22279047, 52102260).

References

[1] H.Q. Fu, M. Zhou, P.F. Liu, P. Liu, H. Yin, K.Z. Sun, H.G. Yang, M. Al-Mamun, P. Hu, H.F. Wang, H. Zhao, Hydrogen spillover-bridged volmer/tafel processes enabling ampere-level current density alkaline hydrogen evolution reaction under low overpotential, J. Am. Chem. Soc. 144 (2022) 6028–6039.

[2] Y. Zhang, F. Gao, D. Wang, Z. Li, X. Wang, C. Wang, K. Zhang, Y. Du, Amorphous/crystalline heterostructure transition-metal-based catalysts for high-performance water splitting, Coord. Chem. Rev. 475 (2023), 214916.

[3] F. Gao, Y. Zhang, F. Ren, Y. Shiraishi, Y. Du, Universal surfactant-free strategy for self-standing 3D tremella-Like Pd-M (M = Ag, Pb, and Au) nanosheets for superior alcohols electrocatalysis, Adv. Funct. Mater. 30 (2020), 2000255.

[4] X. Xiao, L. Zou, H. Pang, Q. Xu, Synthesis of micro/nanoscaled metal-organic frameworks and their direct electrochemical applications, Chem. Soc. Rev. 49 (2020) 301–331.

[5] Y. Zhang, Z. Li, K. Zhang, Z. Wu, F. Gao, Y. Du, Heterogeneous interface engineering for boosting electron transfer induced by MOF-derived Yolk-shell trimetallic phosphide nanospindles for robust water oxidation electrocatalysis, Appl. Surf. Sci. 590 (2022), 153102.

[6] F. Gao, Y. Zhang, Z. Wu, H. You, Y. Du, Universal strategies to multi-dimensional noble-metal-based catalysts for electrocatalysis, Coord. Chem. Rev. 436 (2021), 213825.

[7] M. Wang, N. Zhang, Y. Feng, Z. Hu, Q. Shao, X. Huang, Partially pyrolyzed binary metal-organic framework nanosheets for efficient electrochemical hydrogen peroxide synthesis, Angew. Chem. Int. Ed. 59 (2020) 14373–14377.

[8] T. Zhu, J. Huang, B. Huang, N. Zhang, S. Liu, Q. Yao, S.C. Haw, Y.C. Chang, C. W. Pao, J.M. Chen, Q. Shao, Z. Hu, Y. Ma, X. Huang, High-index faceted RuCo nanoscrews for water electrosplitting, Adv. Energy Mater. 10 (2020), 2002860.

[9] W. Zheng, L.Y.S. Lee, Metal–organic frameworks for electrocatalysis: catalyst or precatalyst? ACS Energy Lett. 6 (2021) 2838–2843.

[10] X. Liu, J. Meng, J. Zhu, M. Huang, B. Wen, R. Guo, L. Mai, Comprehensive understandings into complete reconstruction of precatalysts: synthesis, applications, and characterizations, Adv. Mater. 33 (2021), 2007344.

[11] Y. Zhang, D. Wang, C. Ye, F. Gao, Z. Li, Y. Du, Regulation of crystallinity and defects on $CoNiRuO_x$ nanocages for enhanced oxygen evolution reaction, Chem. Eng. J. 466 (2023), 143059.

[12] X. Liu, W. Li, X. Zhao, Y. Liu, C.W. Nan, L.Z. Fan, Two birds with one stone: metal–organic framework derived micro-/nanostructured Ni2P/Ni hybrids embedded in porous carbon for electrocatalysis and energy storage, Adv. Funct. Mater. 29 (2019), 1901510.

[13] L. Zhai, T.W. Benedict Lo, Z.-L. Xu, J. Potter, J. Mo, X. Guo, C.C. Tang, S.C. Edman Tsang, S.P. Lau, In situ phase transformation on nickel-based selenides for enhanced hydrogen evolution reaction in alkaline medium, ACS Energy Lett. 5 (2020) 2483–2491.

[14] C. Cao, D.D. Ma, J. Jia, Q. Xu, X.T. Wu, Q.L. Zhu, Divergent paths, same goal: a pair-electrosynthesis tactic for cost-efficient and exclusive formate production by metal-organic-framework-derived 2D electrocatalysts, Adv. Mater. 33 (2021), 2008631.

[15] A. Meena, P. Thangavel, D.S. Jeong, A.N. Singh, A. Jana, H. Im, D.A. Nguyen, K. S. Kim, Crystalline-amorphous interface of mesoporous $Ni_2P@FePO_xH_y$ for oxygen evolution at high current density in alkaline-anion-exchange-membrane water-electrolyzer, Appl. Catal. B Environ. 306 (2022), 121127.

[16] P. Thangavel, G. Kim, K.S. Kim, Electrochemical integration of amorphous NiFe (oxy)hydroxides on surface-activated carbon fibers for high-efficiency oxygen evolution in alkaline anion exchange membrane water electrolysis, J. Mater. Chem. A 9 (2021) 14043–14051.

[17] Y. Zhang, F. Gao, H. You, Z. Li, B. Zou, Y. Du, Recent advances in one-dimensional noble-metal-based catalysts with multiple structures for efficient fuel-cell electrocatalysis, Coord. Chem. Rev. 450 (2022), 214244.

[18] J. Su, R. Ge, K. Jiang, Y. Dong, F. Hao, Z. Tian, G. Chen, L. Chen, Assembling ultrasmall copper-doped ruthenium oxide nanocrystals into hollow porous polyhedra: highly robust electrocatalysts for oxygen evolution in acidic media, Adv. Mater. 30 (2018), 1801351.

[19] D. Hu, J.-Q. Zhang, X. Wang, J. Song, X. Lin, H. Ren, One-pot synthesis of pompon-like bimetallic organic framework for enhanced oxygen evolution electrocatalysis, J. Power Sources 520 (2022), 230812.

[20] W. Shao, M. Xiao, C. Yang, M. Cheng, S. Cao, C. He, M. Zhou, T. Ma, C. Cheng, S. Li, Assembling and regulating of transition metal-based heterophase vanadates as efficient oxygen evolution catalysts, Small 18 (2022), 2105763.

[21] C. Wei, Y. Sun, G.G. Scherer, A.C. Fisher, M. Sherburne, J.W. Ager, Z.J. Xu, Surface composition dependent ligand effect in tuning the activity of nickel-copper bimetallic electrocatalysts toward hydrogen evolution in alkaline, J. Am. Chem. Soc. 142 (2020) 7765–7775.

[22] X. Zheng, Y. Qian, H. Gong, W. Shi, J. Yan, W. Wang, X. Guo, J. Zhang, X. Cao, R. Yang, Bridge-linking interfacial engineering of triple carbons for highly efficient and binder-free electrodes toward flexible Zn-air batteries, Appl. Catal. B-Environ. 319 (2022), 121937.

[23] J. Yang, L. Xu, W. Zhu, M. Xie, F. Liao, T. Cheng, Z. Kang, M. Shao, Rh/RhO_x nanosheets as pH-universal bifunctional catalysts for hydrazine oxidation and hydrogen evolution reactions, J. Mater. Chem. A 10 (2022) 1891–1898.

[24] Z. Gong, R. Liu, H. Gong, G. Ye, J. Liu, J. Dong, J. Liao, M. Yan, J. Liu, K. Huang, L. Xing, J. Liang, Y. He, H. Fei, Constructing a graphene-encapsulated amorphous/crystalline heterophase NiFe alloy by microwave thermal shock for boosting the oxygen evolution reaction, ACS Catal. 11 (2021) 12284–12292.

[25] L. Zhong, X. Wang, Y. Guo, J. Ding, Q. Huang, T.T. Li, Y. Hu, J. Qian, S. Huang, Differentiated oxygen evolution behavior in MOF-derived oxide nanomaterials induced by phase transition, ACS Appl. Mater. Inter. 13 (2021) 55454–55462.

[26] Z. Liu, F. Zheng, W. Xiong, X. Li, A. Yuan, H. Pang, Strategies to improve electrochemical performances of pristine metal-organic frameworks-based electrodes for lithium/sodium-ion batteries, SmartMat 2 (2021) 488–518.

[27] X. Li, M. Hou, X. Qu, Y. Zhang, M. Li, Electric-field assisted hydrolysis-oxidation of MOFs: hierarchical ternary (oxy)hydroxide micro-flowers for efficient electrocatalytic oxygen evolution, Small 18 (2022), 2104863.

[28] Z. Zhuang, Y. Wang, C.Q. Xu, S. Liu, C. Chen, Q. Peng, Z. Zhuang, H. Xiao, Y. Pan, S. Lu, R. Yu, W.C. Cheong, X. Cao, K. Wu, K. Sun, Y. Wang, D. Wang, J. Li, Y. Li, Three-dimensional open nano-netcage electrocatalysts for efficient pH-universal overall water splitting, Nat. Commun. 10 (2019) 4875.

[29] J. Wu, Z. Yu, Y. Zhang, S. Niu, J. Zhao, S. Li, P. Xu, Understanding the effect of second metal on CoM (M = Ni, Cu, Zn) metal-organic frameworks for electrocatalytic oxygen evolution reaction, Small 17 (2021), 2105150.

[30] H. Xu, X. Niu, Z. Liu, M. Sun, Z. Liu, Z. Tian, X. Wu, B. Huang, Y. Tang, C.H. Yan, Highly controllable hierarchically porous Ag/Ag_2S heterostructure by cation exchange for efficient hydrogen evolution, Small 17 (2021), 2103064.

[31] C. Chen, W. Zhang, H. Zhu, B.-G. Li, Y. Lu, S. Zhu, Fabrication of metal-organic framework-based nanofibrous separator via one-pot electrospinning strategy, Nano Res 14 (2020) 1465–1470.
[32] K. Zhan, C. Feng, X. Feng, D. Zhao, S. Yue, Y. Li, Q. Jiao, H. Li, Y. Zhao, Iron-doped nickel cobalt phosphide nanoarrays with urchin-like structures as high-performance electrocatalysts for oxygen evolution reaction, ACS Sustain. Chem. Eng. 8 (2020) 6273–6281.
[33] W. Zhou, Z. Xue, Q. Liu, Y. Li, J. Hu, G. Li, Trimetallic MOF-74 films grown on Ni foam as bifunctional electrocatalysts for overall water splitting, ChemSusChem 13 (2020) 5647–5653.
[34] S. Luo, R. Gu, P. Shi, J. Fan, Q. Xu, Y. Min, π-π interaction boosts catalytic oxygen evolution by self-supporting metal-organic frameworks, J. Power Sources 448 (2020), 227406.
[35] Z. Xu, C.L. Yeh, Y. Jiang, X. Yun, C.T. Li, K.C. Ho, J.T. Lin, R.Y. Lin, Orientation-adjustable metal-organic framework nanorods for efficient oxygen evolution reaction, ACS Appl. Mater. Inter. 13 (2021) 28242–28251.
[36] J. Liang, X. Gao, B. Guo, Y. Ding, J. Yan, Z. Guo, E.C.M. Tse, J. Liu, Ferrocene-based metal-organic framework nanosheets as a robust oxygen, Evol. Catal. Angew. Chem. Int. Ed. 60 (2021) 12770–12774.
[37] Z. Li, X. Zhang, Y. Kang, C.C. Yu, Y. Wen, M. Hu, D. Meng, W. Song, Y. Yang, Interface engineering of Co-LDH@MOF heterojunction in highly stable and efficient oxygen evolution reaction, Adv. Sci. 8 (2021), 2002631.
[38] F.L. Li, Q. Shao, X. Huang, J.P. Lang, Nanoscale trimetallic metal-organic frameworks enable efficient oxygen evolution electrocatalysis, Angew. Chem. Int. Ed. 57 (2018) 1888–1892.
[39] L. Zhuang, L. Ge, H. Liu, Z. Jiang, Y. Jia, Z. Li, D. Yang, R.K. Hocking, M. Li, L. Zhang, X. Wang, X. Yao, Z. Zhu, A. surfactant-free and scalable general strategy for synthesizing ultrathin two-dimensional metal-organic framework nanosheets for the oxygen evolution reaction, Angew. Chem. Int. Ed. 58 (2019) 13565–13572.
[40] Y. Sun, S. Ding, S. Xu, J. Duan, S. Chen, Metallic two-dimensional metal-organic framework arrays for ultrafast water splitting, J. Power Sources 494 (2021), 229733.
[41] Y. Jia, Z. Xu, L. Li, S. Lin, Formation of NiFe-MOF nanosheets on Fe foam to achieve advanced electrocatalytic oxygen evolution, Dalton Trans. 51 (2022) 5053–5060.
[42] X. Sun, X. Zhang, Y. Li, Y. Xu, H. Su, W. Che, J. He, H. Zhang, M. Liu, W. Zhou, W. Cheng, Q. Liu, In situ construction of flexible VNi redox centers over Ni-based MOF nanosheet arrays for electrochemical water oxidation, Small Methods 5 (2021), 2100573.
[43] A. De Vos, K. Hendrickx, P. Van Der Voort, V. Van Speybroeck, K. Lejaeghere, Missing linkers: an alternative pathway to UiO-66 electronic structure engineering, Chem. Mater. 29 (2017) 3006–3019.
[44] Z. Jiang, L. Ge, L. Zhuang, M. Li, Z. Wang, Z. Zhu, Fine-tuning the coordinatively unsaturated metal sites of metal-organic frameworks by plasma engraving for enhanced electrocatalytic activity, ACS Appl. Mater. Inter. 11 (2019) 44300–44307.
[45] C. Liu, J. Wang, J. Wan, Y. Cheng, R. Huang, C. Zhang, W. Hu, G. Wei, C. Yu, Amorphous metal-organic framework-dominated nanocomposites with both compositional and structural heterogeneity for oxygen, Evol. Angew. Chem. Int. Ed. 59 (2020) 3630–3637.
[46] Z. Xue, K. Liu, Q. Liu, Y. Li, M. Li, C.Y. Su, N. Ogiwara, H. Kobayashi, H. Kitagawa, M. Liu, G. Li, Missing-linker metal-organic frameworks for oxygen evolution reaction, Nat. Commun. 10 (2019) 5048.
[47] L. Zhang, X. Wang, A. Li, X. Zheng, L. Peng, J. Huang, Z. Deng, H. Chen, Z. Wei, Rational construction of macroporous CoFeP triangular plate arrays from bimetal–organic frameworks as high-performance overall water-splitting catalysts, J. Mater. Chem. A 7 (2019) 17529–17535.
[48] Y. Xu, S. Yu, T. Ren, S. Liu, Z. Wang, X. Li, L. Wang, H. Wang, Hydrophilic/aerophobic hydrogen-evolving electrode: NiRu-based metal-organic framework nanosheets in situ grown on conductive substrates, ACS Appl. Mater. Inter. 12 (2020) 34728–34735.
[49] W. Li, S. Xue, S. Watzele, S. Hou, J. Fichtner, A.L. Semrau, L. Zhou, A. Welle, A. S. Bandarenka, R.A. Fischer, Advanced bifunctional oxygen reduction and evolution electrocatalyst derived from surface-mounted metal-organic frameworks, Angew. Chem. Int. Ed. 59 (2020) 5837–5843.
[50] Z. Zou, T. Wang, X. Zhao, W.-J. Jiang, H. Pan, D. Gao, C. Xu, Expediting in-situ electrochemical activation of two-dimensional metal-organic frameworks for enhanced OER intrinsic activity by iron incorporation, ACS Catal. 9 (2019) 7356–7364.
[51] Z. Li, M. Hu, P. Wang, J. Liu, J. Yao, C. Li, Heterojunction catalyst in electrocatalytic water splitting, Coord. Chem. Rev. 439 (2021), 213953.
[52] X. Cai, F. Peng, X. Luo, X. Ye, J. Zhou, X. Lang, M. Shi, Understanding the evolution of cobalt-based metal-organic frameworks in electrocatalysis for the oxygen evolution reaction, ChemSusChem 14 (2021) 3163–3173.
[53] D. Yang, Y. Chen, Z. Su, X. Zhang, W. Zhang, K. Srinivas, Organic carboxylate-based MOFs and derivatives for electrocatalytic water oxidation, Coord. Chem. Rev. 428 (2021), 213619.
[54] S. Li, Y. Gao, N. Li, L. Ge, X. Bu, P. Feng, Transition metal-based bimetallic MOFs and MOF-derived catalysts for electrochemical oxygen evolution reaction, Energy Environ. Sci. 14 (2021) 1897–1927.
[55] B. Zhang, Y. Zheng, T. Ma, C. Yang, Y. Peng, Z. Zhou, M. Zhou, S. Li, Y. Wang, C. Cheng, Designing MOF nanoarchitectures for electrochemical water splitting, Adv. Mater. 33 (2021), 2006042.
[56] K. Rui, G. Zhao, Y. Chen, Y. Lin, Q. Zhou, J. Chen, J. Zhu, W. Sun, W. Huang, S. X. Dou, Hybrid 2D dual-metal–organic frameworks for enhanced water oxidation catalysis, Adv. Funct. Mater. 28 (2018), 1801554.
[57] C. Liu, Q. Sun, L. Lin, J. Wang, C. Zhang, C. Xia, T. Bao, J. Wan, R. Huang, J. Zou, C. Yu, Ternary MOF-on-MOF heterostructures with controllable architectural and compositional complexity via multiple selective assembly, Nat. Commun. 11 (2020) 4971.
[58] Q. Zha, F. Yuan, G. Qin, Y. Ni, Cobalt-Based MOF-on-MOF two-dimensional heterojunction nanostructures for enhanced oxygen evolution reaction electrocatalytic activity, Inorg. Chem. 59 (2020) 1295–1305.
[59] T. Bao, Y. Xia, J. Lu, C. Zhang, J. Wang, L. Yuan, Y. Zhang, C. Liu, C. Yu, A. Pacman-Like, Titanium-doped cobalt sulfide hollow superstructure for electrocatalytic oxygen evolution, Small 18 (2022), 2103106.
[60] Z. Gu, X. Wei, X. Zhang, Z. Duan, Z. Gu, Q. Gong, K. Luo, Bimetallic-MOF-derived amorphous zinc/cobalt-iron-based hollow nanowall arrays via ion exchange for highly efficient oxygen evolution, Small 17 (2021), 2104125.
[61] J. Liu, G. Qian, T. Yu, J. Chen, C. Zhu, Y. Li, J. He, L. Luo, S. Yin, Amorphous-crystalline heterostructure for simulated practical water splitting at high-current–density, Chem. Eng. J. 431 (2022), 134247.
[62] M. Zhang, Y. Zhang, L. Ye, B. Guo, Y. Gong, Hierarchically constructed Ag nanowires shelled with ultrathin Co-LDH nanosheets for advanced oxygen evolution reaction, Appl. Catal. B Environ. 298 (2021), 120601.
[63] L. Ye, J. Wang, Y. Zhang, M. Zhang, X. Jing, Y. Gong, A self-supporting electrode with in-situ partial transformation of Fe-MOF into amorphous NiFe-LDH for efficient oxygen evolution reaction, Appl. Surf. Sci. 556 (2021), 149781.
[64] H. Sun, L. Chen, Y. Lian, W. Yang, L. Lin, Y. Chen, J. Xu, D. Wang, X. Yang, M. H. Rummerli, J. Guo, J. Zhong, Z. Deng, Y. Jiao, Y. Peng, S. Qiao, Topotactically transformed polygonal mesopores on ternary layered double hydroxides exposing under-coordinated metal centers for accelerated water dissociation, Adv. Mater. 32 (2020), 2006784.
[65] Y. Wang, S. Wang, Z.L. Ma, L.T. Yan, X.B. Zhao, Y.Y. Xue, J.M. Huo, X. Yuan, S. N. Li, Q.G. Zhai, Competitive coordination-oriented monodispersed ruthenium sites in conductive MOF/LDH hetero-nanotree catalysts for efficient overall water splitting in alkaline media, Adv. Mater. 34 (2022), 2107488.
[66] F. Zheng, W. Zhang, X. Zhang, Y. Zhang, W. Chen, Sub-2 nm ultrathin and robust 2D FeNi layered double hydroxide nanosheets packed with 1D FeNi-MOFs for enhanced oxygen evolution electrocatalysis, Adv. Funct. Mater. 31 (2021), 2103318.
[67] J. Ding, T. Fan, K. Shen, Y. Li, Electrochemical synthesis of amorphous metal hydroxide microarrays with rich defects from MOFs for efficient electrocatalytic water oxidation, Appl. Catal. B Environ. 292 (2021), 120174.
[68] M. Huo, B. Wang, C. Zhang, S. Ding, H. Yuan, Z. Liang, J. Qi, M. Chen, Y. Xu, W. Zhang, H. Zheng, R. Cao, 2D metal-organic framework derived CuCo alloy nanoparticles encapsulated by nitrogen-doped carbonaceous nanoleaves for efficient bifunctional oxygen electrocatalyst and zinc-air batteries, Chemistry 25 (2019) 12780–12788.
[69] C. Zhang, P. Wang, W. Li, Z. Zhang, J. Zhu, Z. Pu, Y. Zhao, S. Mu, MOF-assisted synthesis of octahedral carbon-supported PtCu nanoalloy catalysts for an efficient hydrogen evolution reaction, J. Mater. Chem. A 8 (2020) 19348–19356.
[70] B. Chen, D. Kim, Z. Zhang, M. Lee, K. Yong, MOF-derived NiCoZnP nanoclusters anchored on hierarchical N-doped carbon nanosheets array as bifunctional electrocatalysts for overall water splitting, Chem. Eng. J. 422 (2021), 130533.
[71] Y. Lv, J.R. Gong, In situ growth of MOF-derived ultrafine molybdenum carbide nanoparticles supported on Ni foam as efficient hydrogen-evolution electrocatalysts, J. Mater. Chem. A 9 (2021) 15246–15253.
[72] N. Zhang, Q. Shao, P. Wang, X. Zhu, X. Huang, Porous Pt-Ni nanowires within in situ generated metal-organic frameworks for highly chemoselective cinnamaldehyde hydrogenation, Small 14 (2018), 1704318.
[73] M. Zhao, W. Li, J. Li, W. Hu, C.M. Li, Strong electronic interaction enhanced electrocatalysis of metal sulfide clusters embedded metal-organic framework ultrathin nanosheets toward highly efficient overall water splitting, Adv. Sci. 7 (2020), 2001965.
[74] K. Rui, G. Zhao, M. Lao, P. Cui, X. Zheng, X. Zheng, J. Zhu, W. Huang, S.X. Dou, W. Sun, Direct hybridization of noble metal nanostructures on 2D metal-organic framework nanosheets to catalyze hydrogen evolution, Nano Lett. 19 (2019) 8447–8453.
[75] Z. Xia, J. Fang, X. Zhang, L. Fan, A.J. Barlow, T. Lin, S. Wang, G.G. Wallace, G. Sun, X. Wang, Pt nanoparticles embedded metal-organic framework nanosheets: A synergistic strategy towards bifunctional oxygen electrocatalysis, Appl. Catal. B-Environ. 245 (2019) 389–398.
[76] M. Wang, Y. Xu, C.K. Peng, S.Y. Chen, Y.G. Lin, Z. Hu, L. Sun, S. Ding, C.W. Pao, Q. Shao, X. Huang, Site-specified two-dimensional heterojunction of Pt nanoparticles/metal-organic frameworks for enhanced hydrogen evolution, J. Am. Chem. Soc. 143 (2021) 16512–16518.
[77] H. Lei, S. Yang, Q. Wan, L. Ma, M.S. Javed, S. Tan, Z. Wang, W. Mai, Coordination and interface engineering to boost catalytic property of two-dimensional ZIFs for wearable Zn-air batteries, J. Energy Chem. 68 (2022) 78–86.
[78] C.-L. Zhang, Y. Xie, J.-T. Liu, F.-H. Cao, H.-P. Cong, H. Li, 1D Core−Shell MOFs derived CoP Nanoparticles-Embedded N-doped porous carbon nanotubes anchored with MoS_2 nanosheets as efficient bifunctional electrocatalysts, Chem. Eng. J. 419 (2021), 129977.
[79] Y. Chen, L. Shen, C. Wang, S. Feng, N. Zhang, K. Zhang, B. Yang, Utilizing tannic acid and polypyrrle to induce reconstruction to optimize the activity of MOF-derived electrocatalyst for water oxidation in seawater, Chem. Eng. J. 430 (2022), 132632.

[80] Y. Chen, L. Shen, C. Wang, S. Feng, N. Zhang, S. Xiang, T. Feng, M. Yang, K. Zhang, B. Yang, Utilizing in-situ polymerization of pyrrole to fabricate composited hollow nanospindles for boosting oxygen evolution reaction, Appl. Catal. B-Environ. 274 (2020), 119112.

[81] J. Hu, Y. Qin, H. Sun, Y. Ma, L. Lin, Y. Peng, J. Zhong, M. Chen, X. Zhao, Z. Deng, Combining multivariate electrospinning with surface MOF functionalization to construct tunable active sites toward trifunctional electrocatalysis, Small 18 (2022), 2106260.

[82] S. Chen, M. Li, M. Zhang, C. Wang, R. Luo, X. Yan, H. Zhang, J. Qi, X. Sun, J. Li, Metal organic framework derived one-dimensional porous Fe/N-doped carbon nanofibers with enhanced catalytic performance, J. Hazard. Mater. 416 (2021), 126101.

[83] B. Dahal, S.-H. Chae, A. Muthurasu, T. Mukhiya, J. Gautam, K. Chhetri, S. Subedi, G.P. Ojha, A.P. Tiwari, J.H. Lee, H.-Y. Kim, An innovative synthetic approach for core-shell multiscale hierarchically porous boron and nitrogen codoped carbon nanofibers for the oxygen reduction reaction, J. Power Sources 453 (2020), 227883.

[84] H. Zhong, M. Wang, G. Chen, R. Dong, X. Feng, Two-dimensional conjugated metal-organic frameworks for electrocatalysis: opportunities and challenges, ACS Nano 16 (2022) 1759–1780.

[85] G.-l Zhuang, Y.-f Gao, X. Zhou, X.-y Tao, J.-m Luo, Y.-j Gao, Y.-l Yan, P.-y Gao, X. Zhong, J.-g Wang, ZIF-67/COF-derived highly dispersed Co_3O_4/N-doped porous carbon with excellent performance for oxygen evolution reaction and Li-ion batteries, Chem. Eng. J. 330 (2017) 1255–1264.

[86] S. Wu, Y. Pan, H. Lin, L. Li, X. Fu, J. Long, Crystalline covalent organic frameworks with tailored linkages for photocatalytic H_2 evolution, ChemSusChem 14 (2021) 4958–4972.

[87] Y. Peng, M. Zhao, B. Chen, Z. Zhang, Y. Huang, F. Dai, Z. Lai, X. Cui, C. Tan, H. Zhang, Hybridization of MOFs and COFs: a new strategy for construction of MOF@COF core-shell hybrid materials, Adv. Mater. 30 (2018), 1705454.

[88] Z. Liang, H.Y. Wang, H. Zheng, W. Zhang, R. Cao, Porphyrin-based frameworks for oxygen electrocatalysis and catalytic reduction of carbon dioxide, Chem. Soc. Rev. 50 (2021) 2540–2581.

[89] H.-Y. Zhang, Y. Yang, C.-C. Li, H.-L. Tang, F.-M. Zhang, G.-L. Zhang, H. Yan, A new strategy for constructing covalently connected MOF@COF core–shell heterostructures for enhanced photocatalytic hydrogen evolution, J. Mater. Chem. A 9 (2021) 16743–16750.

[90] Y. Gao, C. Liu, W. Zhou, S. Lu, B. Zhang, Anion vacancy engineering in electrocatalytic water splitting, ChemNanoMat 7 (2020) 102–109.

[91] K. Feng, D. Zhang, F. Liu, H. Li, J. Xu, Y. Xia, Y. Li, H. Lin, S. Wang, M. Shao, Z. Kang, J. Zhong, Highly Efficient oxygen evolution by a thermocatalytic process cascaded electrocatalysis over sulfur-treated Fe-based metal–organic-frameworks, Adv. Energy Mater. 10 (2020), 2000184.

[92] B. Yuan, C. Li, L. Guan, K. Li, Y. Lin, Prussian blue analog nanocubes tuning synthesis of coral-like Ni_3S_2@MIL-53(NiFeCo) core-shell nanowires array and boosting oxygen evolution reaction, J. Power Sources 451 (2020), 227295.

[93] Y.J. Lee, S.K. Park, Metal-organic framework-derived hollow CoSx nanoarray coupled with NiFe layered double hydroxides as efficient bifunctional electrocatalyst for overall water splitting, Small 18 (2022), 2200586.

[94] G. Anandhababu, Y. Huang, D.D. Babu, M. Wu, Y. Wang, Oriented growth of ZIF-67 to derive 2D porous CoPO nanosheets for electrochemical-/photovoltage-driven overall water splitting, Adv. Funct. Mater. 28 (2018), 1706120.

[95] D. Wu, D. Chen, J. Zhu, S. Mu, Ultralow Ru incorporated amorphous cobalt-based oxides for high-current-density overall water splitting in alkaline and seawater media, Small 17 (2021), 2102777.

[96] M. Wang, M. Zhang, W. Song, L. Zhou, X. Wang, Y. Tang, Heteroatom-doped amorphous cobalt-molybdenum oxides as a promising catalyst for robust hydrogen evolution, Inorg. Chem. 61 (2022) 5033–5039.

[97] X.-Y. Zhang, Y.-R. Zhu, Y. Chen, S.-Y. Dou, X.-Y. Chen, B. Dong, B.-Y. Guo, D.-P. Liu, C.-G. Liu, Y.-M. Chai, Hydrogen evolution under large-current-density based on fluorine-doped cobalt-iron phosphides, Chem. Eng. J. 399 (2020), 125831.

[98] X. Guo, M. Duan, J. Zhang, B. Xi, M. Li, R. Yin, X. Zheng, Y. Liu, F. Cao, X. An, S. Xiong, A general self-assembly induced strategy for synthesizing 2D ultrathin cobalt-based compounds toward optimizing hydrogen evolution catalysis, Adv. Funct. Mater. (2022), 2209397.

[99] Y. Yao, S. Hu, W. Chen, Z.-Q. Huang, W. Wei, T. Yao, R. Liu, K. Zang, X. Wang, G. Wu, W. Yuan, T. Yuan, B. Zhu, W. Liu, Z. Li, D. He, Z. Xue, Y. Wang, X. Zheng, J. Dong, C.-R. Chang, Y. Chen, X. Hong, J. Luo, S. Wei, W.-X. Li, P. Strasser, Y. Wu, Y. Li, Engineering the electronic structure of single atom Ru sites via compressive strain boosts acidic water oxidation electrocatalysis, Nat. Catal. 2 (2019) 304–313.

[100] S.L. Zhang, B.Y. Guan, X.F. Lu, S. Xi, Y. Du, X.W.D. Lou, Metal atom-doped Co_3O_4 hierarchical nanoplates for electrocatalytic oxygen evolution, Adv. Mater. 32 (2020), 2002235.

[101] C. Wang, L. Qi, Heterostructured inter-doped ruthenium-cobalt oxide hollow nanosheet arrays for highly efficient overall water splitting, Angew. Chem. Int. Ed. 59 (2020) 17219–17224.

[102] K. Huang, Y. Sun, Y. Zhang, X. Wang, W. Zhang, S. Feng, Hollow-structured metal oxides as oxygen-related catalysts, Adv. Mater. 31 (2019), 1801430.

[103] C. Chen, Y. Tuo, Q. Lu, H. Lu, S. Zhang, Y. Zhou, J. Zhang, Z. Liu, Z. Kang, X. Feng, D. Chen, Hierarchical trimetallic Co-Ni-Fe oxides derived from core-shell structured metal-organic frameworks for highly efficient oxygen evolution reaction, Appl. Catal. B Environ. 287 (2021), 119953.

[104] Q. Qian, Y. Li, Y. Liu, G. Zhang, General anion-exchange reaction derived amorphous mixed-metal oxides hollow nanoprisms for highly efficient water oxidation electrocatalysis, Appl. Catal. B Environ. 266 (2020), 118642.

[105] X. Yin, R. Cai, X. Dai, F. Nie, Y. Gan, Y. Ye, Z. Ren, Y. Liu, B. Wu, Y. Cao, X. Zhang, Electronic modulation and surface reconstruction of cactus-like CoB_2O_4@FeOOH heterojunctions for synergistically triggering oxygen evolution reactions, J. Mater. Chem. A 10 (2022) 11386.

[106] J. Chi, H. Yu, B. Qin, L. Fu, J. Jia, B. Yi, Z. Shao, Vertically aligned FeOOH/NiFe layered double hydroxides electrode for highly efficient oxygen evolution reaction, ACS Appl. Mater. Inter. 9 (2017) 464–471.

[107] Z. Shi, Z. Yu, R. Jiang, J. Huang, Y. Hou, J. Chen, Y. Zhang, H. Zhu, B. Wang, H. Pang, MOF-derived M-OOH with rich oxygen defects by in situ electro-oxidation reconstitution for a highly efficient oxygen evolution reaction, J. Mater. Chem. A 9 (2021) 11415–11426.

[108] Y. Cui, Y. Xue, R. Zhang, J. Zhang, Xa Li, X. Zhu, Vanadium–cobalt oxyhydroxide shows ultralow overpotential for the oxygen evolution reaction, J. Mater. Chem. A 7 (2019) 21911–21917.

[109] G. Li, Y. Sun, J. Rao, J. Wu, A. Kumar, Q.N. Xu, C. Fu, E. Liu, G.R. Blake, P. Werner, B. Shao, K. Liu, S. Parkin, X. Liu, M. Fahlman, S.C. Liou, G. Auffermann, J. Zhang, C. Felser, X. Feng, Carbon-tailored semimetal MoP as an efficient hydrogen evolution electrocatalyst in both alkaline and acid media, Adv. Energy Mater. 8 (2018), 1801258.

[110] Q. Hu, X. Huang, Z. Wang, G. Li, Z. Han, H. Yang, X. Ren, Q. Zhang, J. Liu, C. He, Unconventionally fabricating defect-rich NiO nanoparticles within ultrathin metal–organic framework nanosheets to enable high-output oxygen evolution, J. Mater. Chem. A 8 (2020) 2140–2146.

[111] Q. Yu, J. Chi, G. Liu, X. Wang, X. Liu, Z. Li, Y. Deng, X. Wang, L. Wang, Dual-strategy of hetero-engineering and cation doping to boost energy-saving hydrogen production via hydrazine-assisted seawater electrolysis, Sci. China Mater. 65 (2022) 1539–1549.

[112] Y. Sun, S. Xu, C.A. Ortíz-Ledón, J. Zhu, S. Chen, J. Duan, Biomimetic assembly to superplastic metal–organic framework aerogels for hydrogen evolution from seawater electrolysis, Exploration 1 (2021), 20210021.

[113] H.-S. Hu, Y. Li, Y.-R. Shao, K.-X. Li, G. Deng, C.-B. Wang, Y.-Y. Feng, NiCoP nanorod arrays as high-performance bifunctional electrocatalyst for overall water splitting at high current densities, J. Power Sources 484 (2021), 229269.

[114] C. Wang, L. Qi, Hollow nanosheet arrays assembled by ultrafine ruthenium–cobalt phosphide nanocrystals for exceptional pH-universal hydrogen evolution, ACS Mater. Lett. 3 (2021) 1695–1701.

[115] W. He, R. Ifraemov, A. Raslin, I. Hod, Room-temperature electrochemical conversion of metal-organic frameworks into porous amorphous metal sulfides with tailored composition and hydrogen evolution Activity, Adv. Funct. Mater. 28 (2018), 1707244.

[116] Z. Su, J. Zhang, J. Jin, S. Yang, G. Li, Nanoscale surface modification of polymer nanofibers enables uniform lithium nucleation and deposition for stable lithium metal anodes, Chem. Eng. J. 430 (2022), 132865.

[117] B. Yu, F. Qi, B. Zheng, W. Hou, W. Zhang, Y. Li, Y. Chen, Self-assembled pearl-bracelet-like $CoSe_2$–$SnSe_2$/CNT hollow architecture as highly efficient electrocatalysts for hydrogen evolution reaction, J. Mater. Chem. A 6 (2018) 1655–1662.

[118] X. Wang, B. Zheng, B. Yu, B. Wang, W. Hou, W. Zhang, Y. Chen, In situ synthesis of hierarchical $MoSe_2$–$CoSe_2$ nanotubes as an efficient electrocatalyst for the hydrogen evolution reaction in both acidic and alkaline media, J. Mater. Chem. A 6 (2018) 7842–7850.

[119] P. Liu, J. Yan, J. Mao, J. Li, D. Liang, W. Song, In-plane intergrowth CoS_2/MoS_2 nanosheets: binary metal–organic framework evolution and efficient alkaline HER electrocatalysis, J. Mater. Chem. A 8 (2020) 11435–11441.

[120] J. Zhang, W. He, H.B. Aiyappa, T. Quast, S. Dieckhöfer, D. Öhl, J.R.C. Junqueira, Y.T. Chen, J. Masa, W. Schuhmann, Hollow CeO_2@Co_2N nanosheets derived from Co-ZIF-L for boosting the oxygen evolution reaction, Adv. Mater. Inter. 8 (2021), 2100041.

[121] Y. Pan, K. Sun, S. Liu, X. Cao, K. Wu, W.C. Cheong, Z. Chen, Y. Wang, Y. Li, Y. Liu, D. Wang, Q. Peng, C. Chen, Y. Li, Core-Shell ZIF-8@ZIF-67-derived CoP nanoparticle-embedded N-doped carbon nanotube hollow polyhedron for efficient overall water splitting, J. Am. Chem. Soc. 140 (2018) 2610–2618.

[122] J. Jiang, P. Jiang, D. Wang, Y. Li, The synthetic strategies for single atomic site catalysts based on metal-organic frameworks, Nanoscale 12 (2020) 20580–20589.

[123] Y. Chen, P. Wang, H. Hao, J. Hong, H. Li, S. Ji, A. Li, R. Gao, J. Dong, X. Han, M. Liang, D. Wang, Y. Li, Thermal atomization of platinum nanoparticles into single atoms: an effective strategy for engineering high-performance nanozymes, J. Am. Chem. Soc. 143 (2021) 18643–18651.

[124] L. Zou, Y.S. Wei, C.C. Hou, C. Li, Q. Xu, Single-atom catalysts derived from metal-organic frameworks for electrochemical applications, Small 17 (2021), 2004809.

[125] Y.S. Wei, M. Zhang, R. Zou, Q. Xu, Metal-organic framework-based catalysts with single metal sites, Chem. Rev. 120 (2020) 12089–12174.

[126] X. Zhang, S. Zhang, Y. Yang, L. Wang, Z. Mu, H. Zhu, X. Zhu, H. Xing, H. Xia, B. Huang, J. Li, S. Guo, E. Wang, A General method for transition metal single atoms anchored on honeycomb-like nitrogen-doped carbon nanosheets, Adv. Mater. 32 (2020), 1906905.

[127] W. Chen, J. Pei, C.T. He, J. Wan, H. Ren, Y. Wang, J. Dong, K. Wu, W.C. Cheong, J. Mao, X. Zheng, W. Yan, Z. Zhuang, C. Chen, Q. Peng, D. Wang, Y. Li, Single tungsten atoms supported on MOF-derived N-doped carbon for robust electrochemical hydrogen evolution, Adv. Mater. 30 (2018), 1800396.

[128] Y. Hu, G. Luo, L. Wang, X. Liu, Y. Qu, Y. Zhou, F. Zhou, Z. Li, Y. Li, T. Yao, C. Xiong, B. Yang, Z. Yu, Y. Wu, Single Ru Atoms stabilized by hybrid amorphous/

crystalline FeCoNi layered double hydroxide for ultraefficient oxygen evolution, Adv. Energy Mater. 11 (2020), 2002816.
[129] G. Dey, A. Shadab, Aijaz, Metal-organic framework derived nanostructured bifunctional electrocatalysts for water splitting, Chemelectrochem 8 (2021) 3782–3803.
[130] J. Du, F. Li, L. Sun, Metal-organic frameworks and their derivatives as electrocatalysts for the oxygen evolution reaction, Chem. Soc. Rev. 50 (2021) 2663–2695.
[131] L.-M. Cao, D. Lu, D.-C. Zhong, T.-B. Lu, Prussian blue analogues and their derived nanomaterials for electrocatalytic water splitting, Coord. Chem. Rev. 407 (2020), 213156.
[132] H. Zhang, J. Su, K. Zhao, L. Chen, RecenT Advances in Metal-organic Frameworks and Their Derived Materials for Electrocatalytic Water Splitting, Chemelectrochem 7 (2020) 1805–1824.
[133] J. Ye, M. Teng, X. Qian, C. Wan, G. He, H. Chen, A novel MOF-derived strategy to construct Cu-doped CeO_2 supported PdCu alloy electrocatalysts for hydrogen evolution reaction, J. Ind. Eng. Chem. 120 (2023) 96–102.
[134] Q. Yuan, Y. Yu, P.C. Sherrell, J. Chen, X. Bi, Fe/Co-based bimetallic MOF-derived Co_3Fe_7 @NCNTFs bifunctional electrocatalyst for high-efficiency overall water splitting, Chem. -Asian J. 15 (2020) 1728–1735.
[135] Y. Luo, Z. Zhang, M. Chhowalla, B. Liu, Recent advances in design of electrocatalysts for high-current-density water splitting, Adv. Mater. 34 (2022), 2108133.
[136] N.K. Dang, J.N. Tiwari, S. Sultan, A. Meena, K.S. Kim, Multi-site catalyst derived from Cr atoms-substituted CoFe nanoparticles for high-performance oxygen evolution activity, Chem. Eng. J. 404 (2021), 126513.
[137] A. Meena, P. Thangavel, A.S. Nissimagoudar, A. Narayan Singh, A. Jana, D. Sol Jeong, H. Im, K.S. Kim, Bifunctional oxovanadate doped cobalt carbonate for high-efficient overall water splitting in alkaline-anion-exchange-membrane water-electrolyzer, Chem. Eng. J. 430 (2022), 132623.
[138] Z. Dong, F. Lin, Y. Yao, L. Jiao, Crystalline $Ni(OH)_2$/amorphous NiMoOxmixed-catalyst with Pt-like performance for hydrogen production, Adv. Energy Mater. 9 (2019), 1902703.
[139] S. Zhao, C. Tan, C.-T. He, P. An, F. Xie, S. Jiang, Y. Zhu, K.-H. Wu, B. Zhang, H. Li, J. Zhang, Y. Chen, S. Liu, J. Dong, Z. Tang, Structural transformation of highly active metal–organic framework electrocatalysts during the oxygen evolution reaction, Nat. Energy 5 (2020) 881–890.
[140] P. Yan, Y. Hu, E. Shoko, T.T. Isimjan, J. Tian, X. Yang, Hierarchical core-shell N-doped carbon@FeP_4-CoP arrays as robust bifunctional electrocatalysts for overall water splitting at high current density, Adv. Mater. Inter. 8 (2021), 2100065.
[141] M.A. Ahsan, T. He, K. Eid, A.M. Abdullah, M.F. Sanad, A. Aldalbahi, B. Alvarado-Tenorio, A. Du, A.R. Puente Santiago, J.C. Noveron, Controlling the interfacial charge polarization of MOF-derived 0D–2D vdW architectures as a unique strategy for bifunctional oxygen electrocatalysis, ACS Appl. Mater. Inter. 14 (2022) 3919–3929.
[142] M. Li, H. Sun, J. Yang, M. Humayun, L. Li, X. Xu, X. Xue, A. Habibi-Yangjeh, K. Temst, C. Wang, Mono-coordinated metallocene ligands endow metal-organic frameworks with highly efficient oxygen evolution and urea electrolysis, Chem. Eng. J. 430 (2022), 132733.
[143] L. Meng, L. Zhang, Y. Zhu, H. Jiang, Y.V. Kaneti, J. Na, Y. Yamauchi, D. Golberg, H. Jiang, C. Li, Highly dispersed secondary building unit-stabilized binary metal center on a hierarchical porous carbon matrix for enhanced oxygen evolution reaction, Nanoscale 13 (2021) 1213–1219.
[144] X. Gu, Z. Liu, H. Liu, C. Pei, L. Feng, Fluorination of ZIF-67 framework templated Prussian blue analogue nano-box for efficient electrochemical oxygen evolution reaction, Chem. Eng. J. 403 (2021), 126371.
[145] J. Zhou, Z. Han, X. Wang, H. Gai, Z. Chen, T. Guo, X. Hou, L. Xu, X. Hu, M. Huang, S.V. Levchenko, H. Jiang, Discovery of quantitative electronic structure-OER activity relationship in metal-organic framework electrocatalysts using an integrated theoretical-experimental approach, Adv. Funct. Mater. 31 (2021), 2102066.
[146] G. Zhou, P. Wang, H. Li, B. Hu, Y. Sun, R. Huang, L. Liu, Spin-sate reconfiguration induced by alternating magnetic field for efficient oxygen evolution reaction, Nat. Commun. 12 (2021) 4827.
[147] D. Senthil Raja, H.-W. Lin, S.-Y. Lu, Synergistically well-mixed MOFs grown on nickel foam as highly efficient durable bifunctional electrocatalysts for overall water splitting at high current densities, Nano Energy 57 (2019) 1–13.
[148] C.-P. Wang, Y. Feng, H. Sun, Y. Wang, J. Yin, Z. Yao, X.-H. Bu, J. Zhu, Self-optimized metal–organic framework electrocatalysts with structural stability and high current tolerance for water oxidation, ACS Catal. 11 (2021) 7132–7143.
[149] Z. Zou, J. Wang, H. Pan, J. Li, K. Guo, Y. Zhao, C. Xu, Enhanced oxygen evolution reaction of defective CoP/MOF-integrated electrocatalyst by partial phosphating, J. Mater. Chem. A 8 (2020) 14099–14105.
[150] T. Kang, J. Kim, Optimal cobalt-based catalyst containing high-ratio of oxygen vacancy synthesized from metal-organic-framework (MOF) for oxygen evolution reaction (OER) enhancement, Appl. Surf. Sci. 560 (2021), 150035.
[151] J. Ren, M. Ledwaba, N.M. Musyoka, H.W. Langmi, M. Mathe, S. Liao, W. Pang, Structural defects in metal–organic frameworks (MOFs): Formation, detection and control towards practices of interests, Coord. Chem. Rev. 349 (2017) 169–197.
[152] H. Huang, H. Kim, A. Lee, S. Kim, W.-G. Lim, C.-Y. Park, S. Kim, S.-K. Kim, J. Lee, Structure engineering defective and mass transfer-enhanced RuO_2 nanosheets for proton exchange membrane water electrolyzer, Nano Energy 88 (2021), 106276.
[153] M. Wu, J. Zhao, C. Li, R. Liu, Heterogeneity in a metal–organic framework in situ guides engineering Co@CoO heterojunction for electrocatalytic H_2 production in tandem with glucose oxidation, J. Mater. Chem. A 10 (2022) 4791–4799.
[154] H. Xu, J. Cao, C. Shan, B. Wang, P. Xi, W. Liu, Y. Tang, MOF-DErived Hollow CoS decorated with CeOx nanoparticles for boosting oxygen evolution reaction electrocatalysis, Angew. Chem. Int. Ed. 57 (2018) 8654–8658.
[155] Z. Lei, X. Jin, J. Li, Y. Liu, J. Liu, S. Jiao, R. Cao, Tuning electrochemical transformation process of zeolitic imidazolate framework for efficient water oxidation activity, J. Energy Chem. 65 (2022) 505–513.
[156] X. Mu, H. Yuan, H. Jing, F. Xia, J. Wu, X. Gu, C. Chen, J. Bao, S. Liu, S. Mu, Superior electrochemical water oxidation in vacancy defect-rich 1.5 nm ultrathin trimetal-organic framework nanosheets, Appl. Catal. B-Environ. 296 (2021), 120095.
[157] W. Li, Y. Niu, X. Wu, F. Wu, T. Li, W. Hu, Heterostructured $CoSe_2$/$FeSe_2$ nanoparticles with abundant vacancies and strong electronic coupling supported on carbon nanorods for oxygen evolution electrocatalysis, ACS Sustain. Chem. Eng. 8 (2020) 4658–4666.
[158] N. Yao, R. Meng, F. Wu, Z. Fan, G. Cheng, W. Luo, Oxygen-vacancy-induced CeO_2/Co_4N heterostructures toward enhanced pH-Universal hydrogen evolution reactions, Appl. Catal. B-Environ. 277 (2020), 119282.
[159] L. Zhang, H. Jang, H. Liu, M.G. Kim, D. Yang, S. Liu, X. Liu, J. Cho, Sodium-decorated amorphous/crystalline RuO_2 with rich oxygen vacancies: a robust pH-universal oxygen evolution electrocatalyst, Angew. Chem. Int. Ed. 60 (2021) 18821–18829.
[160] B. Wang, X. Han, C. Guo, J. Jing, C. Yang, Y. Li, A. Han, D. Wang, J. Liu, Structure inheritance strategy from MOF to edge-enriched NiFe-LDH array for enhanced oxygen evolution reaction, Appl. Catal. B Environ. 298 (2021), 120580.
[161] X. Wang, J. He, B. Yu, B. Sun, D. Yang, X. Zhang, Q. Zhang, W. Zhang, L. Gu, Y. Chen, $CoSe_2$ nanoparticles embedded MOF-derived Co-N-C nanoflake arrays as efficient and stable electrocatalyst for hydrogen evolution reaction, Appl. Catal. B-Environ. 258 (2019), 117996.
[162] P. Thangavel, M. Ha, S. Kumaraguru, A. Meena, A.N. Singh, A.M. Harzandi, K. S. Kim, Graphene-nanoplatelets-supported NiFe-MOF: high-efficiency and ultra-stable oxygen electrodes for sustained alkaline anion exchange membrane water electrolysis, Energy Environ. Sci. 13 (2020) 3447–3458.
[163] L. Wu, F. Zhang, S. Song, M. Ning, Q. Zhu, J. Zhou, G. Gao, Z. Chen, Q. Zhou, X. Xing, T. Tong, Y. Yao, J. Bao, L. Yu, S. Chen, Z. Ren, Efficient alkaline water/seawater hydrogen evolution by a nanorod-nanoparticle-structured Ni-MoN catalyst with fast water-dissociation kinetics, Adv. Mater. 34 (2022), 2201774.
[164] Z. Sun, X. Cao, M. Tian, K. Zeng, Y. Jiang, M.H. Rummeli, P. Strasser, R. Yang, Synergized multimetal oxides with amorphous/crystalline heterostructure as efficient electrocatalysts for lithium–oxygen batteries, Adv. Energy Mater. 11 (2021), 2100110.
[165] M. Kuang, J. Zhang, D. Liu, H. Tan, K.N. Dinh, L. Yang, H. Ren, W. Huang, W. Fang, J. Yao, X. Hao, J. Xu, C. Liu, L. Song, B. Liu, Q. Yan, Amorphous/crystalline heterostructured cobalt-vanadium-iron (Oxy)hydroxides for highly efficient oxygen evolution reaction, Adv. Energy Mater. 10 (2020), 2002215.
[166] D. Senthil Raja, X.-F. Chuah, S.-Y. Lu, In situ grown bimetallic MOF-based composite as highly efficient bifunctional electrocatalyst for overall water splitting with ultrastability at high current densities, Adv. Energy Mater. 8 (2018), 1801065.
[167] Y. Ge, P. Dong, S.R. Craig, P.M. Ajayan, M. Ye, J. Shen, Transforming nickel hydroxide into 3D Prussian Blue analogue array to obtain Ni_2P/Fe_2P for efficient hydrogen evolution reaction, Adv. Energy Mater. 8 (2018), 1800484.
[168] F.-Y. Chen, Z.-Y. Wu, Z. Adler, H. Wang, Stability challenges of electrocatalytic oxygen evolution reaction: From mechanistic understanding to reactor design, Joule 5 (2021) 1704–1731.
[169] R. Zhu, J. Ding, Y. Xu, J. Yang, Q. Xu, H. Pang, pi-conjugated molecule boosts metal-organic frameworks as efficient oxygen evolution reaction catalysts, Small 14 (2018), 1803576.
[170] T.I. Singh, G. Rajeshkhanna, U.N. Pan, T. Kshetri, H. Lin, N.H. Kim, J.H. Lee, Alkaline water splitting enhancement by MOF-derived Fe-Co-Oxide/Co@NC-mNS heterostructure: boosting OER and HER through Defect Engineering and in Situ Oxidation, Small 17 (2021), 2101312.
[171] K. Wan, J. Luo, C. Zhou, T. Zhang, J. Arbiol, X. Lu, B.W. Mao, X. Zhang, J. Fransaer, Hierarchical porous Ni_3S_4 with enriched high-valence Ni sites as a robust electrocatalyst for efficient oxygen evolution reaction, Adv. Funct. Mater. 29 (2019), 1900315.
[172] J.X. Feng, S.H. Ye, H. Xu, Y.X. Tong, G.R. Li, Design and synthesis of FeOOH/CeO_2 heterolayered nanotube electrocatalysts for the oxygen evolution reaction, Adv. Mater. 28 (2016) 4698–4703.
[173] W.H. Choi, K.H. Kim, H. Lee, J.W. Choi, D.G. Park, G.H. Kim, K.M. Choi, J. K. Kang, Metal-organic fragments with adhesive excipient and their utilization to stabilize multimetallic electrocatalysts for high activity and robust durability in oxygen evolution reaction, Adv. Sci. 8 (2021), 2100044.
[174] G. Zhang, J. Zeng, J. Yin, C. Zuo, P. Wen, H. Chen, Y. Qiu, Iron-facilitated surface reconstruction to in-situ generate nickel–iron oxyhydroxide on self-supported FeNi alloy fiber paper for efficient oxygen evolution reaction, Appl. Catal. B-Environ. 286 (2021), 119902.
[175] J. Wang, J. Hu, S. Niu, S. Li, Y. Du, P. Xu, Crystalline-amorphous $Ni_2P_4O_{12}$/$NiMoO_x$ nanoarrays for alkaline water electrolysis: enhanced catalytic activity via in situ surface reconstruction, Small 18 (2022), 2105972.
[176] L. Wu, L. Yu, F. Zhang, B. McElhenny, D. Luo, A. Karim, S. Chen, Z. Ren, Heterogeneous bimetallic phosphide Ni_2P-Fe_2P as an efficient bifunctional catalyst for water/seawater splitting, Adv. Funct. Mater. 31 (2020), 2006484.
[177] H. Jiang, Q. He, Y. Zhang, L. Song, Structural self-reconstruction of catalysts in electrocatalysis, Acc. Chem. Res 51 (2018) 2968–2977.

[178] N.C.S. Selvam, L. Du, B.Y. Xia, P.J. Yoo, B. You, Reconstructed water oxidation electrocatalysts: the impact of surface dynamics on intrinsic activities, Adv. Funct. Mater. 31 (2020), 2008190.
[179] S. Chen, L. Ma, Z. Huang, G. Liang, C. Zhi, In situ/operando analysis of surface reconstruction of transition metal-based oxygen evolution electrocatalysts, Cell Rep. Phys. Sci. 3 (2022), 100729.
[180] D. Yang, Z. Su, Y. Chen, K. Srinivas, X. Zhang, W. Zhang, H. Lin, Self-reconstruction of a MOF-derived chromium-doped nickel disulfide in electrocatalytic water oxidation, Chem. Eng. J. 430 (2022), 133046.
[181] R.-Y. Fan, J.-Y. Xie, H.-J. Liu, H.-Y. Wang, M.-X. Li, N. Yu, R.-N. Luan, Y.-M. Chai, B. Dong, Directional regulating dynamic equilibrium to continuously update electrocatalytic interface for oxygen evolution reaction, Chem. Eng. J. 431 (2022), 134040.
[182] B. Xu, Y. Zhang, Y. Pi, Q. Shao, X. Huang, Research progress of nickel-based metal-organic frameworks and their derivatives for oxygen evolution catalysis, Acta Phys. Chim. Sin. (2020), 2009074-2009070.
[183] L. An, C. Wei, M. Lu, H. Liu, Y. Chen, G.G. Scherer, A.C. Fisher, P. Xi, Z.J. Xu, C. H. Yan, Recent development of oxygen evolution electrocatalysts in acidic environment, Adv. Mater. 33 (2021), 2006328.